



Vaasan yliopisto
UNIVERSITY OF VAASA

Mohammad Sadegh Moosavi

A Simulation Study of Renewable-Energy-Integrated Building Energy Systems

School of Technology and Innovations

Master's Thesis

Master's Thesis in Electrical and Energy Engineering

Vaasa 2026

UNIVERSITY OF VAASA
School of Technology and Innovations

Author:	Mohammad Sadegh Moosavi		
Title of the thesis:	A Simulation Study of Renewable-Energy-Integrated Building Energy Systems		
Degree:	Master of Science in Technology and Innovations		
Degree Programme:	Master's Programme in Electrical and Energy Engineering		
Supervisor:	Professor Xiaoshu Lu		
Instructor:	Anne Mäkiranta		
Year:	2026	Pages:	96

ABSTRACT:

Heating, Ventilation, and Air Conditioning (HVAC) systems account for a substantial portion of building energy consumption. Given the high energy use and associated carbon emissions, implementing solutions that improve energy efficiency, achieve carbon neutrality, and integrate renewable energy is crucial. Among renewable sources, geothermal energy provides a sustainable option, particularly in cold climates such as those in the Nordic countries.

The primary objective of this thesis is to simulate an integrated building energy system for a representative office building to determine the energy required to meet the building's thermal load and to analyze the temporal temperature variations in boreholes over time. Optimization is also employed to evaluate how borehole depth influences the coefficient of performance (COP) of the Water Source Heat Pump (WSHP). For this purpose, an office building was selected for simulation.

A lumped-zone energy model of the building was developed, and a three-dimensional model of the building was constructed in SketchUp and imported into TRNSYS using the multi-zone building component. The building's envelope, thermal capacitance, infiltration rate, ventilation rate, and internal gains (including occupants, equipment, and lighting) were modeled according to ASHRAE standards and actual building documentation using TRNBuild. Simulations were conducted for one year to estimate heating and cooling loads, which were then linked to a water-source heat pump. Thermal performance in the boreholes was assessed to evaluate both short-term seasonal temperature variation and long-term thermal balance.

The results indicate that the water-source heat pump and borehole system can effectively provide heating and cooling. The soil temperature decreases during winter and increases during summer, and the boreholes gradually reach a long-term thermal balance between heat extraction and injection after several years of operation. Overall, the building's total simulated energy demand was slightly higher than the measured data.

This study demonstrates that integrating geothermal heat pumps with borehole heat exchangers is an energy-efficient and environmentally sustainable solution for large buildings in cold climates. The findings highlight the importance of accurate modeling of building loads and ground interactions to ensure reliable long-term performance.

KEYWORDS: BES, WSHP, BHE, TRNSYS, HVAC, COP, RES

Acknowledgment

This research was conducted as part of a 30-credit Master's thesis in Electrical and Energy Engineering (Major: Smart Energy) at the University of Vaasa. The study was carried out between May 2025 and October 2025. This work received financial support from the ProLight project, funded by the Horizon Europe programme (Grant No. 101079902).

AI tools were used solely for language editing and proofreading. All modeling, analysis, and interpretation were conducted independently by the author.

This thesis was completed under the supervision of Professor Xiaoshu Lu at the University of Vaasa, with guidance and support from Instructor Dr. Anne Mäkiranta. The author gratefully acknowledges their valuable comments, supervision, and academic support throughout the research process.

Vaasa, 2025

Mohammad Sadegh Moosavi

Contents

1	Introduction	9
2	Literature Review	12
2.1	Structure and Scope of the Literature Review	12
2.2	Energy Crisis and Sustainable Building Goals	13
2.3	The Role of Integrated Renewable Energy Systems in Commercial Buildings	15
2.3.1	Overview of Key Technologies	17
2.3.2	Challenges in System Design and Integration	18
2.4	Physics of Dynamic Building Energy Simulation	20
2.4.1	The Energy Balance Equation	22
2.4.2	Components of Energy Balance (Heat Losses and Gains)	24
2.4.3	Physical Model to Control-Oriented Model	26
2.4.4	The Role of Thermal Mass	28
2.5	Building Energy Simulation (BES) Tools and Methodologies	29
2.5.1	Overview of Major Simulation Engines	31
2.5.2	TRNSYS: A Modular Simulation Environment	34
2.5.3	Justification for Tool Selection	36
2.6	Review of Previous Studies on Load Analysis and Modeling	37
2.6.1	Studies on Model Calibration and Validation	38
2.6.2	Studies on Sensitivity Analysis of Building Parameters	39
2.6.3	Case Studies of Commercial/Institutional Buildings in Cold Climates	40

2.7	Identifying the Research Gap and Objectives	42
3	Research Method	44
3.1	Building Energy Model Development	46
3.2	Internal Gains	54
3.3	Internal Capacitance:	58
3.4	Infiltration	59
3.5	Ventilation Air	59
3.6	Heating and Cooling Load:	63
4	Results and discussion	73
4.1	Temperature Control	73
4.2	Boreholes Temperatures:	75
4.3	Heating and Cooling Mode:	78
5	Optimization of COP of heat pump:	79
6	Validation:	82
7	Component List	84
8	Summary	85
9	Conclusion	87
	References	88

Figures

Figure 1. Global carbon emission trends in the building sector. (A) Proportion of building sector's carbon emissions in 2022. (B) Changes in operational CO₂ emissions from the

building sector, 2010–2070. (C) Contribution of top economies to global building sector CO ₂ emissions in 2010 and 2020. (Ma et al., 2025)	13
Figure 2. Application of BEMS in nZEB (Hannan et al., 2018)	16
Figure 3. Overview of building heat dynamics (Pachano & Bandera, 2021)	21
Figure 4. SketchUp model of the Building with help of TRNSYS3D	46
Figure 5. Importing TRNSYS3D file into TRNBuild	47
Figure 6. TRNBuild simulation Environment	48
Figure 7. Layers and Materials of the external walls	49
Figure 8. Layers and Materials of the external roofs	50
Figure 9. Layers and Materials of the external the ground floor	51
Figure 10. Layers and Materials of the external adjacent walls	52
Figure 11. Layers and Materials of the external windows	53
Figure 12. Adding people’s gain from the program library	55
Figure 13. Definition of lighting gain	56
Figure 14. Lighting and Equipment Gain Schedules (TRNSYS, 2024)	57
Figure 15. Adding ventilation types	61
Figure 16. Definition of heating load	63
Figure 17. Definition of heating load	64
Figure 18. Connection between weather and WSHP	67
Figure 19. Connection 5 stages thermostat and the WSHP	69
Figure 20. Setpoints of the thermostat	69
Figure 21. Setpoints at the building	70
Figure 22. Boreholes	72
Figure 23. Temperature of the zones and the ambient in January	73
Figure 24. Temperature of the zone1 is controlled by WSHP	74
Figure 25. Soil temperatures in boreholes during the first years	75
Figure 26. Soil temperatures in boreholes after 2 years	76
Figure 27. Soil temperatures in boreholes after 3 years	76

Figure 28. Soil temperatures in boreholes after 4 years	77
Figure 29. Soil temperatures in boreholes after 5 years	77
Figure 30. Heating and Cooling Mode	78
Figure 31. Optimization	81
Figure 32. Objective function (cop) vs depth	81

Tables

Table 1. Material of external walls	49
Table 2. Material of external roofs	50
Table 3. Material of external the ground floor	51
Table 4. Equation of gains	57
Table 5. Capacitance of zones	58
Table 6. Infiltration rate	59
Table 7. HVAC settings	62
Table 8. Heating & Cooling Loads	65
Table 9. Optimization results	80
Table 10. Heating loads for each zone	82
Table 11. cooling loads for each zone	82

Abbreviations:

U	building loss coefficient(kJ/hr-m ² -C)
Cap	building capacitance (kJ/C)
C _{air}	specific heat of building air (kJ/kg-C)
ρ _{air}	density of building air (kg/m ³)

Zone (Area)	building surface area (m ²)
Vol	building volume (m ³)
T _{vent}	temperature of ventilation air (C)
m _{vent}	ventilation air mass flow rate (kg/hr)
T _{amb}	ambient temperature (C)
m _{inf}	mass flow rate of infiltration air
Q _{lights}	rate of energy gain from lights (kJ/hr)
Q _{equip}	rate of energy gain from equipment (kJ/hr)
Q _{peop}	rate of sensible energy gain from people (kJ/hr)
T _{zone}	zone temperature (C)
Q _{infls}	sensible energy gain from infiltration (kJ/hr)
Q _{vents}	sensible energy gain from ventilation (kJ/hr)

1 Introduction

Buildings are responsible for a substantial share of global final energy consumption and greenhouse gas emissions, with heating, ventilation, and air conditioning (HVAC) systems accounting for nearly 40% of total building energy use (Z. Wang et al., 2025). As international climate targets increasingly emphasize carbon neutrality and net-zero energy buildings, improving the efficiency and sustainability of building energy systems has become a critical research and engineering challenge.

Among renewable energy technologies, geothermal energy has gained significant attention due to its stability, reliability, and long-term sustainability. Unlike solar and wind energy, which are subject to strong temporal variability, geothermal energy provides a nearly constant heat source throughout the year. This characteristic makes geothermal systems particularly suitable for building applications in cold climates, where heating demand is dominant (Xu et al., 2025). Water source heat pumps (WSHPs) coupled with borehole heat exchangers (BHEs) represent one of the most widely adopted configurations for utilizing shallow geothermal energy for space heating and cooling (Zhang et al., 2025).

Previous studies have demonstrated that borehole-based systems offer several advantages over conventional air-source heat pumps. Due to the relatively stable ground temperature, WSHPs connected to boreholes can operate at higher efficiencies, leading to improved coefficients of performance (COP) and reduced electricity consumption (Cazorla-Marín et al., 2020). In addition, borehole fields can act as seasonal thermal energy storage systems, storing excess heat during summer operation and releasing it during winter, thereby enhancing long-term system balance and sustainability (Kvalsvik et al., 2025). Under optimized operating conditions, borehole heat exchanger systems have been reported to reduce building energy consumption by up to 66% (C. Wang et al., 2025). Vertical U-tube boreholes are especially attractive due to their high thermal performance and limited surface area requirements (X. Wang et al., 2025a).

Despite these advantages, the long-term thermal behavior of borehole fields and their interaction with WSHP systems remain complex and highly dependent on building load profiles, climatic conditions, and system design parameters. In particular, borehole depth selection plays a crucial role in determining system performance, ground temperature evolution, and overall COP. While several studies have investigated borehole systems, there is still a need for detailed, building-specific dynamic simulations that capture long-term interactions between the building, heat pump, and ground.

Dynamic simulation tools provide an effective approach to addressing this challenge. TRNSYS is widely recognized as a reliable and computationally efficient software for modeling building energy systems, including geothermal heat pump applications. Compared to computationally intensive numerical methods, TRNSYS enables faster simulations while maintaining sufficient accuracy for system-level analysis (De Rosa et al., 2015). For borehole modeling, several TRNSYS components have been developed, among which Type 557 has been identified as one of the most capable for simulating vertical borehole heat exchangers under transient conditions (Kirschstein et al., 2025).

The aim of this MSc thesis is to simulate a representative (reference) office building using TRNSYS in order to analyze the dynamic behavior of its energy system with a particular focus on the interaction between a water source heat pump and a borehole heat exchanger field. A detailed digital model of the building is developed to evaluate the response of heating, cooling, and ventilation systems under varying weather conditions, occupancy patterns, and operational scenarios. Key performance indicators such as energy demand and system COP are analyzed to assess overall system performance.

Furthermore, this study specifically investigates the temporal evolution of borehole temperature and its impact on WSHP efficiency. Autodesk Navisworks is used for building measurement and review, SketchUp for geometric modeling, and TRNSYS for dynamic energy simulation. A parametric optimization of borehole depth is conducted to identify the depth that yields the best COP. The results provide insight into the seasonal and long-term

interaction between the borehole field and the WSHP during both heating and cooling operation. The simulations indicate that the borehole field reaches a stable thermal regime after approximately five years of continuous operation, offering valuable guidance for the design and optimization of geothermal energy systems in buildings.

2 Literature Review

2.1 Structure and Scope of the Literature Review

This chapter lays the theoretical and empirical basis for this research by developing, through the literature, a structured argument. The argument is deductive in nature, progressing from the broad, global context right down to the specific research domain of this thesis. The review contextualizes the research in the global energy crisis, determining the critical role of the building sector and establishing Operational Carbon (OC) as the main target for decarbonization (Section 2.2). From this premise, the logical step is to explore Integrated Renewable Energy Systems as the principal solution and their inherent technological and design complexities (Section 2.3).

In order to address such complexities, Section 2.4 introduces Building Energy Modeling BEM as the indispensable methodology for the analysis and optimization of such systems. This is followed by the comparison of simulation tools, leading to the justification of choosing TRNSYS, valued for its modularity and flexibility, in Section 2.5. Having the simulation tool at hand, the next step is a review of the critical practices that ensure a model's credibility, starting with seminal studies on calibration, validation, and sensitivity analysis, as presented in Section 2.6. It is here, finally, that the synthesis of these interwoven themes, from the macro-level problem to the micro-level analytical techniques, leads the review to a clear and defensible identification of the research gap, with the articulation of the exact objectives of this thesis, as presented in Section 2.7.

2.2 Energy Crisis and Sustainable Building Goals

Today's global landscape faces the dual challenges of rising energy demand and climate change, making the building sector crucial for effective decarbonization (Ma et al., 2025). This sector has a significant environmental impact, contributing a large part of total energy use and about 37% of global energy-related carbon dioxide emissions (Cao et al., 2025). The common method to measure this impact over a building's life is the Life Cycle Assessment (LCA), which breaks down the total carbon footprint into two main parts: Embodied Carbon (EC) and Operational Carbon (OC) (Ma et al., 2025), (Cao et al., 2025).

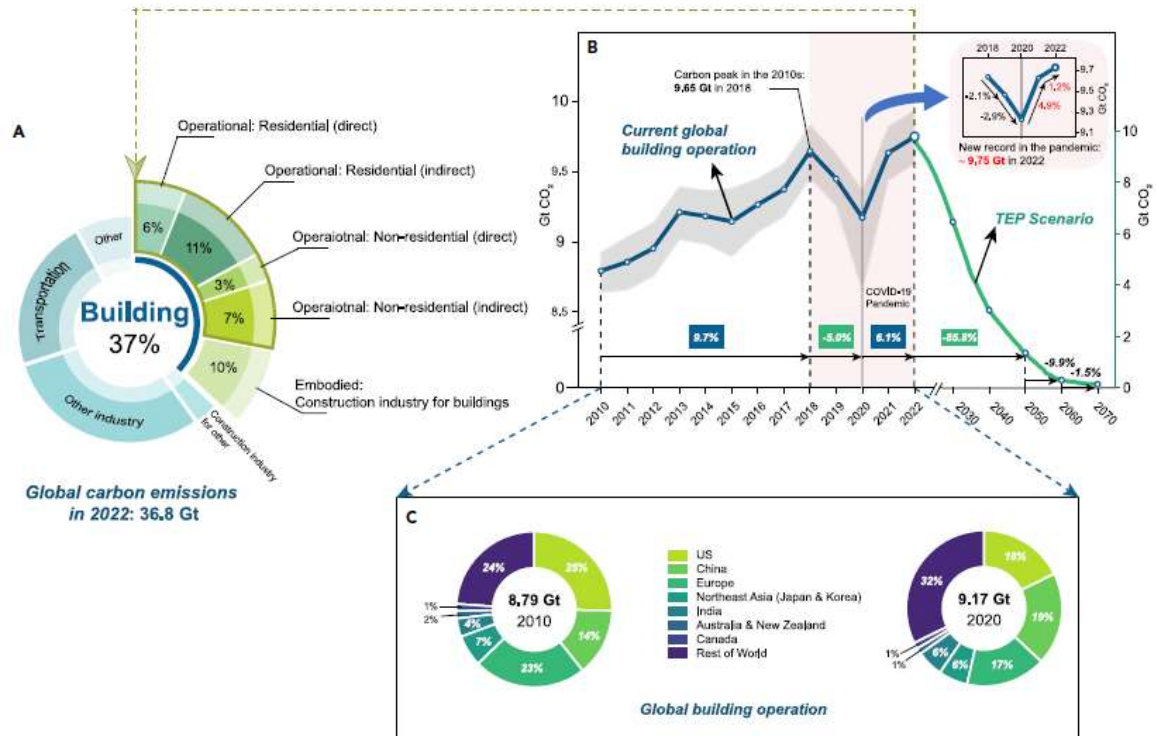


Figure 1. Global carbon emission trends in the building sector. (A) Proportion of building sector's carbon emissions in 2022. (B) Changes in operational CO₂ emissions from the building sector, 2010–2070. (C) Contribution of top economies to global building sector CO₂ emissions in 2010 and 2020. (Ma et al., 2025)

To create effective decarbonization strategies, it's vital to grasp the relative contributions of these components. The latest annual data from 2022 shows that, out of the 37% of total emissions linked to the building sector, Operational Carbon (OC) contributes 27%, which is almost three times greater than the 10% from Embodied Carbon (EC) (see Figure 1). This difference becomes even clearer across a building's entire lifespan, with studies estimating that the operational stage is responsible for over 85% of total lifecycle emissions (Zhao et al., 2025). While it's important to recognize that Life Cycle Assessment results can vary and require building-specific analysis (Fan & Fang, 2023), looking at both annual and lifecycle data firmly positions the operational phase as the main target for impactful interventions. Thus, reducing Operational Carbon (OC) is the key focus of this thesis.

Having identified the operational phase as the primary driver of a building's carbon footprint, we now turn to strategies for its reduction. Although a complete approach should also include measures for Embodied Carbon (EC) through material innovations and Circular Economy (CE) principles [(Amarasinghe et al., 2024), (Finamore & Oltean-Dumbrava, 2024)], OC's significant lifecycle impact calls for a focused effort. The global research community has aligned around a two-pronged strategy: major improvements in energy efficiency and smooth integration of Renewable Energy Sources (RES) (Filali & Chafi, 2025).

However, this strategy has moved beyond passive methods to what is called 'Smart Implementation,' which uses digital tools like AI and BIM to actively manage complex energy flows (Xie & Sun, 2025). This technological shift adds another layer of complexity, illustrated by systems like High-Temperature Borehole Thermal Energy Storage (HT-BTES). A case study in Drammen, Norway, showed that the effectiveness of such systems relies heavily on detailed, precise simulation models (Kvalsvik et al., 2025). This reliance provides an important insight: as sustainable building systems become more integrated and complex, validated, data-driven analysis changes from a design tool to a necessity for operations.

The intricate nature of these systems makes traditional control methods insufficient, leading to the adoption of new approaches like Reinforcement Learning (RL) for optimizing energy performance (Michailidis et al., 2025). However, the success and safety of an RL controller depend on a high-quality, efficient simulation environment. This environment must closely mimic the building's thermodynamic and energy system responses, acting as a crucial foundation for a Digital Twin, a virtual model used for testing, prediction, and control optimization (Michailidis et al., 2025).

This push for advanced modeling is consistently backed by an evolving regulatory framework. The established standard of Nearly Zero-Energy Buildings (NZEBs) has been replaced by the stricter requirement of Zero-Emission Buildings (ZEBs) (Maduta et al., 2025), (Magrini et al., 2020). A key part of the ZEB requirement is the need for zero on-site carbon emissions from fossil fuels. This change means that traditional backups, like natural gas boilers, are no longer viable options (Maduta et al., 2025). The removal of this safety net greatly increases the demand for accurate and reliable system predictions. As a result, creating precise, dynamic building energy models shifts from being an academic pursuit for optimization to being essential for the operational viability of the next generation of sustainable buildings.

2.3 The Role of Integrated Renewable Energy Systems in Commercial Buildings

Commercial buildings are an essential sector for global decarbonization, differing from residential buildings in their very high energy intensity, complex HVAC systems, and unique occupancy patterns. As a result of these atypical operational demands, modern energy and climate pursuits in the commercial building sector to shift the paradigm from deploying standalone components to deeply integrated, intelligent energy ecosystems (Reddy et al., 2024). The challenge today is not just the mere addition of a technology like PV panels,

which alone cannot meet the demands of today (Olatunde et al., 2024), but the integration of a varied portfolio comprising on-site generation, storage, and control systems into one that optimizes performance in real-time (Canale et al., 2021). The basic architecture of this ecosystem is visually captured in Figure 2.



Figure 2. Application of BEMS in nZEB (Hannan et al., 2018)

Although developed for a residential nZEB, the underlying premise of tightly integrating renewables such as solar and geothermal, with energy storage in the form of batteries, using an intelligent BEMS has direct applicability to the commercial sector. The integrated architecture developed is the technological basis for the decarbonization, grid interactivity, and operational resilience of today's commercial building stock (Hannan et al., 2018).

2.3.1 Overview of Key Technologies

Turning a commercial building into a smart energy hub requires synergy among diverse technologies. To add clarity, such technologies can be split into three layers: the physical hardware components, the intelligent control strategies, and the supporting digital infrastructure. Success of the system relies on the integration of these layers towards energy autonomy and grid flexibility.

A. Hardware Infrastructure: Generation and Storage

It is an on-site generation and storage-based system. Whereas the starting point for most is solar photovoltaics, the leading edge of design has moved to BIPV, where the solar cells become part of the building structure. A holistic approach to ensuring resilience would involve diversification of energy sources, hence incorporating GSHP to tap into the stable earth temperatures and hybrid PVT collectors that generate electricity and heat for space efficiency.

Energy storage becomes indispensable given the intermittency of renewable energy sources. Battery Energy Storage Systems are crucial for managing electrical loads and performing peak shaving. However, since heating and cooling dominate commercial energy consumption, Thermal Energy Storage is equally critical for shifting thermal loads using materials such as Phase Change Materials. New Hybrid Energy Storage Systems now combine battery and thermal storage to let the system select the most economical storage medium in real time.

B. Control Strategies: From Rule-Based to AI

Hardware alone is not enough without intelligence. Conventionally, BEMS relied on simple "if-then" logic, so-called Rule-Based Control (RBC). The growing difficulty of today's systems makes rigid RBC increasingly unsuitable. This has driven a shift toward Model Predictive Control (MPC), a strategy that uses mathematical models and forecasts (e.g., weather, prices) to optimize operations in advance (Wang et al., 2023) ,(Liu et al., 2025)

At the same time, data-driven approaches such as Reinforcement Learning are gaining favor. Unlike MPC, RL does not mandate an a priori physics model but instead learns optimal policies directly from operational data (Kozlovska et al., 2023), (Singh et al., 2025). This is also particularly powerful for complex tasks such as HVAC setpoint optimization (Riazul Jannat Eiva et al., 2023) and balancing efficiency with occupant comfort (Hossain et al., 2023), which are hallmarks of buildings that can actively participate in Demand Response programs (Zarate Perez et al., 2023).

C. Digital Infrastructure and Software

Managing such system lifecycles requires a solid digital backbone. During design, the central digital representation is Building Information Modeling (BIM), allowing for coordination and performance simulations (Akbulut et al., 2025), (Tejani & Toshniwal, 2023). In operation, the Digital Twin takes center stage: a high-fidelity virtual replica continuously updated by IoT sensors. This dynamic model is crucial for real-time monitoring and forms a safe environment for training advanced controllers such as RL (Canale et al., 2021), (Constantinou et al., 2023).

Finally, as more and more elements are added to the system, such as PV, batteries, and heat pumps, centralized control becomes computationally cumbersome. This inherent scalability problem is avoided in Multi-Agent Systems. In an MAS architecture (Manfren et al., 2024), each component is autonomously controlled by an intelligent “agent” that can interact with other agents. Since these systems employ a distributed architecture rather than a centralized one, this also enhances robustness and reduces management complexity in large-scale systems (Gholami et al., 2021).

2.3.2. Challenges in System Design and Integration

Translating the vision of an integrated energy ecosystem into reality introduces formidable hurdles. These are not minor roadblocks but fundamental research gaps. To better understand them, they are classified below into technical, computational, and socio-economic challenges.

A. Technical and Physical Integration Challenges

The difficulty begins at the system design level, where determining the appropriate size and technology mix is challenging. The design of systems, such as geothermal pumps, requires extensive knowledge of site-specific conditions (Salhein et al., 2025), whereas overall optimization involves highly uncertain variables, such as climate patterns and economic factors (Yu et al., 2022).

Physical integration is a significant barrier beyond design. Hardware and software from various vendors lack standardized communication protocols, leading to "information silos" (Akbulut et al., 2025), (Tejani & Toshniwal, 2023). It is this fragmentation that complicates installation and prevents the system from operating as a unified, optimized whole.

B. Computational and Control Challenges

Advanced control strategies come with severe computational challenges. Model-based approaches, such as MPC, face the "model-reality gap": inaccuracies in the mathematical model relative to the physical building lead to performance degradations. On the other hand, model-free approaches, such as Reinforcement Learning, are plagued by "sample inefficiency" and require enormous amounts of data to learn through trial-and-error. It is unsafe to "learn by doing" in an actual building, as this may compromise comfort or equipment (Kozlovska et al., 2023), (Singh et al., 2025). Simulations also need extreme accuracy to avoid the "sim-to-real gap during RL agent training" (Constantinou et al., 2023).

Moreover, the system suffers from the “curse of dimensionality” as controllable devices grow, whereby centralized optimization becomes computationally infeasible. Although MAS provides an inherently decentralized approach, the coordination mechanism for independent agents to reach a global optimum remains an active research challenge. Furthermore, Digital Twins rely on high-quality data, but IoT infrastructure in real-world settings often results in sensor failures and network latency that can corrupt control decisions.

C. Socio-Economic and Regulatory Barriers

Even when technical solutions are available, non-technical barriers stand in the way of widespread adoption. Chief among these is the high capital investment required at the outset (Christodoulides et al., 2024). This factor is exacerbated by the relative absence of supportive policy frameworks or market mechanisms that reward building owners for providing value-added grid services, such as demand response (Reddy et al., 2024), (Hannan et al., 2018). Lastly, there is a severe shortage of qualified professionals with the interdisciplinary skill sets needed to design, install, and operate these increasingly complex integrated systems (Olatunde et al., 2024).

2.4 Physics of Dynamic Building Energy Simulation

Addressing the multifaceted challenges of design, integration, and control is impossible without a robust method for predicting how a building will behave under real-world conditions. This is the fundamental role of dynamic Building Energy Simulation (BES). At its core, a dynamic simulation treats the building not as a static object, but as a system in a constant state of flux, continuously responding to external ‘stressing loads’ from weather and internal loads from occupants and equipment, as conceptualized in Figure 3.

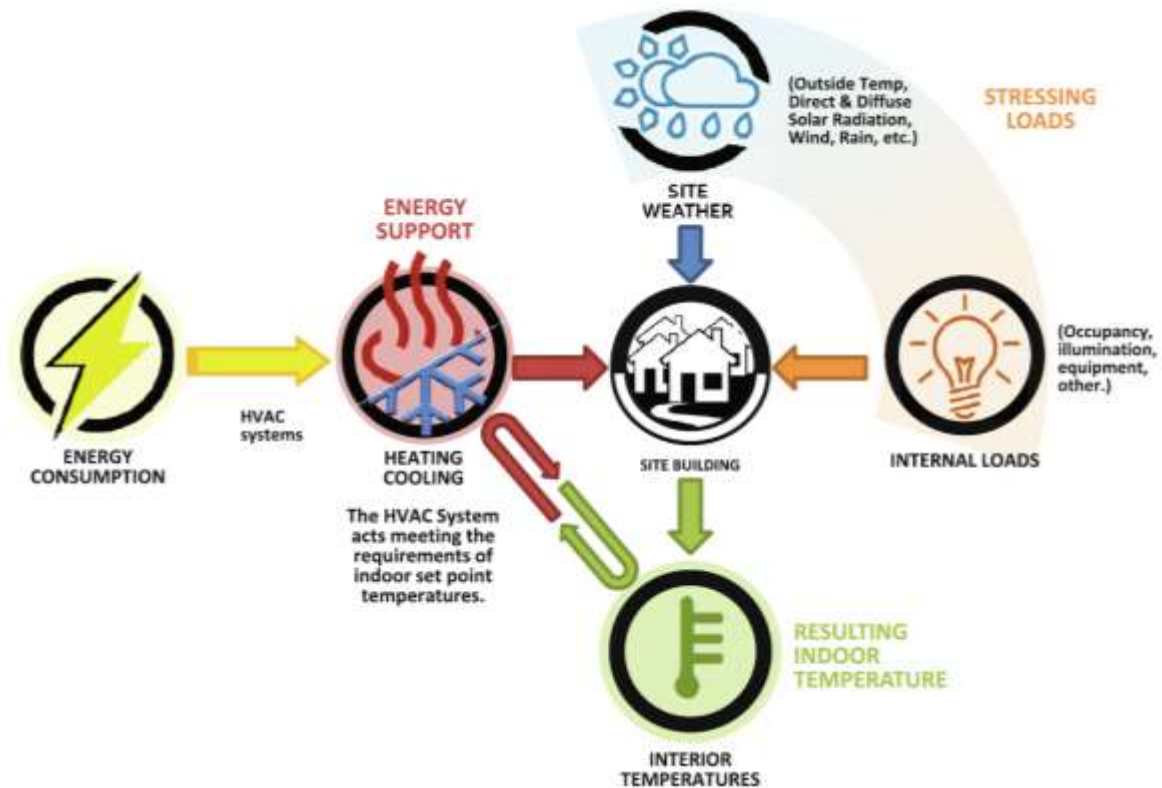


Figure 3. Overview of building heat dynamics (Pachano & Bandera, 2021)

In response to these loads, the HVAC system provides the ‘energy support’ required to counteract these forces and maintain a stable indoor environment. This dynamic approach is what separates modern simulation from older, steady-state methods, which only calculate loads for a single, worst-case scenario. Instead, BES captures the crucial, time-dependent effects of these interactions, especially the ability of the building’s own structure (its thermal mass) to store and release energy over time (Pachano & Bandera, 2021). The entire simulation is anchored in a foundational principle of physics: the conservation of energy. This principle is applied computationally through a detailed energy balance for each zone in the building, which forms the mathematical core of the simulation engine.

2.4.1. The Energy Balance Equation

This principle of energy conservation is mathematically implemented through the heat balance method, which serves as the computational core for leading simulation programs like TRNSYS and EnergyPlus (Barnaby et al., 2005). At any given moment, the method requires that the sum of all heat entering a thermal zone, from surfaces, internal loads, infiltration, and ventilation, must be perfectly balanced by the heat removed by the HVAC system and the energy stored within the zone's air and mass (ASHRAE, 2009).

To enforce this balance at every time step, the simulation engine solves a governing equation for the air within each thermal zone. This equation takes the general form:

$$C_{zone} \frac{dT_{zone}}{dt} = \sum_{i=1}^{N_{surfaces}} \dot{Q}_i + \sum_{j=1}^{N_{loads}} \dot{Q}_j + \dot{Q}_{inf} + \dot{Q}_{vent} + \dot{Q}_{sys} \quad (1)$$

Where:

$C_{zone} \frac{dT_{zone}}{dt}$ is the rate of energy stored in the air mass of the zone (J/s or W).

$\sum_{i=1}^{N_{surfaces}} \dot{Q}_i$ represents the sum of heat transfer from all internal surfaces to the zone air. This term accounts for both convective heat transfer and the net long-wave radiative heat exchange between surfaces.

$\sum_{j=1}^{N_{loads}} \dot{Q}_j$ is the sum of convective heat gains from internal loads such as people, lights, and equipment (W).

\dot{Q}_{inf} is the heat transfer rate due to infiltration of outside air (W).

\dot{Q}_{vent} is the heat transfer rate due to mechanical ventilation (W).

\dot{Q}_{sys} is the rate of heat supplied or extracted by the HVAC system, which represents the heating or cooling load to be met (W).

While the equation itself provides an elegant framework, the ultimate accuracy of the simulation hinges on the fidelity with which each of its constituent terms (the individual heat flows) is calculated. These flows are themselves governed by the complex and interdependent physics of conduction, convection, and radiation. Accurately modeling each of these components, as discussed next, is the central challenge in developing a reliable building model.

B. Latent Heat Balance (Phase Change)

To address the phase change energy mentioned in thermodynamic principles, a separate balance is required for Latent Heat. Unlike sensible heat, latent loads do not change the temperature directly but involve the energy absorbed or released during the phase change of water (vaporization or condensation). Based on the humidity balance method [83], the latent load equation is:

$$\dot{Q}_{Latent_Load} = \dot{Q}_{lat,int} + \dot{Q}_{lat,inf} + \dot{Q}_{lat,vent} \quad (2)$$

These terms are calculated based on the Latent Heat of Vaporization (-), which represents the energy required to change water from liquid to gas phase. The general form for infiltration and ventilation latent loads is:

$$\dot{Q}_{lat} = \dot{m}_{air} \cdot L_v \cdot (q_{outdoor} - q_{zone}) \quad (3)$$

Where:

\dot{m}_{air} is the mass flow rate of air (derived from volumetric flow rate V and density ρ).

L_v is the Latent Heat of Vaporization of water ($\approx 2454\text{kJ/kg}$ at 20°C), representing the energy involved in the phase change process.

q is the specific humidity ratio (kgwater/kgdry_air)

By solving these equations in parallel, the simulation tool determines the total enthalpy change required by the HVAC system, ensuring both thermal comfort (temperature) and air quality (humidity) are maintained.

Heat pumps are typically sized based on cooling demand, with any unmet heating requirements supplied by auxiliary heating. Since humidity effects were not included in the building model, the calculated cooling loads represent sensible loads only. Therefore, heat pump selection should be based on sensible cooling capacity rather than total cooling capacity (TRNSYS, 2024).

2.4.2. Components of Energy Balance (Heat Losses and Gains)

Solving the energy balance equation begins by deconstructing its individual terms. The first component, $\sum \dot{Q}_i$, accounts for the convective heat transfer from the internal surfaces of the envelope. This flow is primarily driven by conduction through opaque elements like walls and roofs.

However, accurately modeling this process requires moving beyond simple one-dimensional analysis. A critical complication arises from thermal bridges, junctions in the building structure, such as wall-to-floor connections or window frame details, that create multi-dimensional heat flow paths. While a traditional steady-state calculation might approximate these with a single, static coefficient, such an approach is inadequate for dynamic simulation. In a real-world scenario where temperatures are in constant flux, static values fail to capture how these complex junctions store and release heat over time. To address this limitation, advanced models employ transfer functions that mathematically describe

the time-dependent behavior of thermal bridges, resulting in a far more accurate estimation of their true impact on building thermal loads (Kim et al., 2022).

The next critical component is the convective heat transfer between the zone's air and its interior surfaces. This is a far more complex phenomenon than conduction through a solid wall. Standard BES tools like TRNSYS typically simplify this by using a lumped-parameter model, which assumes the air in a room is perfectly mixed and has a single, uniform temperature. While computationally efficient, this assumption often breaks down in reality, failing to capture crucial effects like temperature stratification (where warmer air rises) or localized drafts (Kong et al., 2017).

To capture this level of detail, researchers have developed co-simulation methods that couple a BES engine with a Computational Fluid Dynamics (CFD) model. In this powerful hybrid approach, the BES tool continues to manage the building's overall, long-term energy balance, while the CFD model performs a highly detailed, localized simulation of airflow and heat transfer at the surfaces within the room. This division of labor allows each tool to do what it does best, resulting in a much more realistic prediction of the indoor thermal environment and, consequently, the building's true energy performance (Kong et al., 2017).

Finally, the simulation must account for the primary heat gains that drive the need for cooling. Solar radiation transmitted through windows (fenestration) often represents the single largest and most dynamic heat gain, capable of rapidly changing the thermal state of a zone. This is complemented by internal gains from the building's occupants, lighting systems, and equipment. Because these loads are not constant, they are typically modeled using time-based schedules that represent realistic patterns of occupancy and operation, ensuring the simulation reflects the building's actual use throughout the day and year (ASHRAE, 2009).

Beyond the heat that passes through the building's solid materials, the energy balance is also heavily influenced by the air that moves across its boundaries. This air exchange occurs

in two forms: unintentional infiltration and deliberate ventilation. Infiltration refers to the uncontrolled leakage of outside air through cracks and gaps in the building envelope, imposing a constant thermal penalty. Ventilation, on the other hand, is the controlled and necessary supply of fresh air to ensure occupant health and comfort.

Regardless of their origin, both processes introduce a significant thermal load, as this incoming air must be heated or cooled to match the zone's setpoint. The sensible portion of this load, which relates to the change in temperature, is quantified by the following relationship:

$$\dot{Q}_{sensible} = \dot{m}c_p(T_{outdoor} - T_{zone}) \quad (4)$$

Where \dot{m} is the mass flow rate of air and c_p is the specific heat of air (Kong et al., 2017)

2.4.3. Physical Model to Control-Oriented Model

Whereas the energy balance equation (2-1) is a correct description of building zone thermodynamics, it positions the HVAC system's contribution, \dot{Q}_{sys} , as a dependent variable needed to close the balance. As noted above, such a formulation is descriptive rather than prescriptive and is not directly "actionable" for control design. To enable advanced control strategies such as Model Predictive Control (MPC) or Reinforcement Learning (RL), the model needs reformulation in a way that explicitly represents the causal relationship between the actions taken by the controller and the response of the building.

To bridge this gap, the physical model is transformed into a control-oriented state-space representation, which is the standard in modern building control [85]. This involves defining the system's states (x), controllable inputs (u), and uncontrollable disturbances (d):

State Variables (x): These represent the system's memory. The principal state is the zone air temperature (T_{zone}), plus other temperatures relevant to the dynamic capture of the building's thermal mass, such as wall layer and floor slab temperatures.

Control Inputs (u): This is the key step in the transformation. The HVAC quantity, \dot{Q}_{sys} , is not considered as an unknown load to be determined. Instead, it is redefined as the key control input a controller can manipulate within the system to affect its behavior. Therefore, the vector input is specified as $u = [\dot{Q}_{sys}]$.

Disturbance Variables (d): These are external, uncontrollable factors that affect the system, including ambient temperature ($T_{outdoor}$), solar radiation, and scheduled internal gains from occupants and equipment.

With this re-characterization, the dynamic equation 2-1 is conceptually transformed into the standard state-space form ($\frac{dx}{dt} = f(x, u, d)$), which relies on a crucial simplification:

Key Assumption: The HVAC system is modeled as an ideal actuator. This means the supervisory controller is assumed to be able to command a desired heat flow, \dot{Q}_{sys} , directly into the zone. At this stage, the complex internal dynamics of the HVAC plant, such as valve positions and pump curves, are abstracted away to facilitate high-level control design [85].

Such a control-oriented model could have ultimate value by serving as a "virtual testbed" or "source domain" for advanced, data-driven control strategies. As noted in [84], high-fidelity simulations are a necessary ingredient to safely pre-train AI agents, such as those used in Reinforcement Learning, to make the leap from simulation to reality ("Sim-to-Real"). Yet most literature on AI control assumes such a validated physical model is already at hand. That critical, often overlooked, prerequisite is therefore the subject of this thesis. The main contribution of this work is thus not in deploying an AI agent, but rather in the rigorous development and analysis of the foundational TRNSYS simulation itself. In establishing this credible, validated model, the essential, non-negotiable starting point upon which to build and test future intelligent control systems is provided.

2.4.4. The Role of Thermal Mass

So far, our discussion of the energy balance equation has focused on the various heat flows (\dot{Q}). We now turn to the final, crucial element: the energy storage within the building itself, represented by the term $C_{zone} \frac{dT_{zone}}{dt}$. This is the domain of thermal mass the building's inherent ability to act as a thermal sponge. Materials with high thermal mass, like concrete, absorb heat during warm periods and release it slowly as conditions cool. This passive buffering effect naturally dampens indoor temperature swings and, crucially, can both reduce and shift peak heating and cooling loads.

The significance of this load-shifting is not trivial. Dynamic simulation studies, such as one analyzing an office building with varying levels of concrete, have quantified these benefits, demonstrating significant reductions in both annual energy consumption and peak demand. By shifting the time of maximum energy use away from the grid's most stressed and expensive hours, strategic use of thermal mass directly translates to lower operational costs and reduced strain on the utility infrastructure (Andjelkovic et al., 2012).

But the true potential of thermal mass is realized when it is moved from a passive component to an actively controlled asset for demand-side management. By intentionally "pre-cooling" the building's mass during off-peak hours when electricity is cheaper, cooling loads during subsequent peak periods can be dramatically reduced. However, there is a critical prerequisite for this strategy to be effective: a high-performance building envelope. As model-based investigations have shown, without excellent insulation, any stored "coolth" is quickly lost to the outside environment, rendering the pre-cooling strategy useless (Sun et al., 2024). In essence, a well-insulated envelope is the key that unlocks the full load-shifting capability of a building's thermal mass, making the two inseparable components of a high-performance, grid-interactive design.

2.5 Building Energy Simulation (BES) Tools and Methodologies

Building Energy Simulation (BES) tools form the analytical backbone for understanding, predicting, and optimizing the performance of modern buildings—particularly those integrating renewable energy technologies and advanced HVAC systems. As highlighted in previous sections, the transition toward highly efficient, low carbon buildings fundamentally depends on the ability to model not only architectural and thermal loads but also their dynamic interactions with energy generation, storage, and control strategies. BES therefore plays a dual role: first, as the primary tool for evaluating design alternatives, and second, as the foundation for digital platforms (e.g., Digital Twins) used throughout a building’s operational life.

Given the central importance of simulation in such contexts, it is essential to classify the range of modeling approaches available today. These approaches differ in complexity, computational efficiency, and suitability for integration with optimization or advanced control strategies.

(A) Simplified Static Methods

Traditional methods such as Degree Day, Bin, and Monthly energy analyses represent the earliest and simplest form of BES. They rely on aggregated climate indicators (e.g., heating and cooling degree days) and steady state assumptions to estimate annual or monthly energy use. These methods remain useful for early stage sizing, rule of thumb benchmarking, and policy level assessments due to their low input requirements and fast computation. However, their inability to capture transient behavior, interactions among building systems, or the dynamics required for supervisory control makes them unsuitable for detailed performance analysis.

(B) Simplified Dynamic Models (RC / Lumped Approaches)

RC-network or lumped-capacitance models constitute a bridge between simple static methods and full dynamic simulation. These models represent the building envelope and internal mass with resistances and capacitances, capturing transient heat transfer without requiring full geometric detail. Their principal advantage lies in computational efficiency, making them particularly valuable for engineering applications where model simplicity is essential—most notably, Model Predictive Control (MPC) and grey box system identification. Nevertheless, developing accurate RC models often demands extensive calibration, and their limited physical expressiveness restricts their applicability across buildings with complex geometries or non-standard HVAC configurations.

(C) Fully Dynamic, Physics Based Simulation Engines

The most comprehensive category consists of detailed, physics based engines capable of simulating multi zone heat transfer, moisture transport, HVAC equipment dynamics, controls, and interactions with distributed energy resources. These white box tools include EnergyPlus, IDA ICE, DOE 2, ESP r, TRNSYS, and Modelica/Dymola. They enable high resolution analysis of thermal and system behavior, making them indispensable for research on integrated systems, geothermal applications, hybrid energy storage, and demand-side flexibility. Because they capture nonlinearities and cross domain interactions, these tools serve as high fidelity “virtual laboratories” for advanced design and—as demonstrated in recent literature—provide a robust foundation for Digital Twins used in MPC or RL-driven optimization.

Having established this taxonomy, the next subsection reviews the principal simulation engines in more detail while focusing on a key requirement of today’s research landscape: their capability to interact with external controllers, optimization algorithms, and real time decision-making platforms.

2.5.1. Overview of Major Simulation Engines

Given the fundamental role that simulation plays in both design and operation, it is important to compare the major BES engines not only in terms of modeling fidelity but also in terms of extensibility and compatibility with external control frameworks. As highlighted by Rocca Vera et al. (Paola Rocca et al.), existing engines can be broadly classified into special purpose and general purpose tools.

(A) Special Purpose vs General Purpose Simulation Engines

- Special Purpose Engines

These include EnergyPlus, IDA ICE, and DOE 2. They are primarily designed for accurate building thermal simulation grounded in well validated, standardized HVAC models. Their strengths include computational efficiency and reliability, making them ideal for code compliance, retrofit analysis, and standard system evaluation. However, modifying or extending their internal models often proves challenging, particularly when simulating novel technologies or unconventional system architectures.

- General Purpose Engines

TRNSYS and Modelica/Dymola exemplify this category. Their modular architecture allows users to assemble multi domain energy systems, implement custom components, and explore hybrid configurations that go beyond traditional HVAC models. This extensibility makes them particularly suitable for research on geothermal systems, thermal–electrical integration, hybrid storage solutions, or AI assisted control—topics that require flexible and customizable modeling environments.

(B) Profiles of Leading Simulation Engines

- EnergyPlus

EnergyPlus offers highly validated load and HVAC models and supports advanced supervisory logic through the Energy Management System (EMS). Through co simulation frameworks such as BCVTB and FMU/FMI export, EnergyPlus can interact with external MPC implementations. However, recent studies note that its computational burden poses challenges for real time optimization or large scale parametric studies (Cazorla-Marín et al., 2020).

- IDA ICE

IDA ICE excels in accurate indoor climate simulation and system-level HVAC modeling. Its primary limitation is its semi closed architecture, which restricts user customization and makes integration with novel components or non-standard system topologies less straightforward.

- DOE 2

An early-generation but still widely used engine, DOE 2 offers fast steady state time-step simulation but lacks the dynamic and system-integration capabilities required for modern applications such as MPC, RL, or hybrid energy systems analysis.

- ESP r

Known for its rigorous, integrated modeling of building physics, HVAC systems, and electrical networks. Despite its technical strengths, its steep learning curve limits widespread adoption among practitioners.

- Modelica/Dymola

Modelica is a powerful multi-domain modeling environment supporting equation-based simulation of complex energy systems. Its openness and library ecosystem make it a strong candidate for research-intensive applications, although the modeling effort required is significantly higher than for prestructured tools.

- TRNSYS

TRNSYS offers a unique balance between modularity and physical detail, enabling users to assemble systems from existing components or develop custom Types. Its ability to represent hybrid geothermal, solar, electrical, and storage systems makes it particularly suited for integrated energy research. These strengths serve as a natural foundation for Sections 2.5.2 and 2.5.3, which examine TRNSYS performance and validation evidence in depth.

(C) Controller Integration Mechanisms: MPC, RL, and Co Simulation

As building systems evolve toward data-driven, grid-interactive operation, the capability of a simulation engine to interface with external control algorithms becomes a key differentiator. The literature identifies three main integration pathways:

Direct Embedding Within the Simulator

- EnergyPlus via EMS scripting
- TRNSYS via native control Types

These mechanisms are adequate for rule based or schedule driven logic but insufficient for advanced optimal control or learning-based strategies.

Co-Simulation Frameworks

- FMI/FMU (Functional Mock-up Interface)
- BCVTB (Building Controls Virtual Test Bed)
- BOPTTEST, a modern benchmarking environment for MPC/RL

These platforms allow the simulator and controller to exchange data in real time, enabling true closed-loop testing.

External Scripting and API-Based Integration

- TRNSYS–MATLAB coupling (including Type 155) (Meiers & Frey, 2025), (De Rosa et al., 2015)
- TRNSYS–Python interfaces
- EnergyPlus Python API
- Modelica integration with MPC toolboxes

Such interfaces are essential for running optimization, reinforcement learning, or data driven controllers that require flexibility beyond native simulation capabilities.

(D) Relevance to This Thesis

Although this thesis does not implement MPC or RL controllers directly, it contributes the foundational requirement for such future developments: a high fidelity, physics based simulation of an integrated building–geothermal system. As emphasized in recent works by Drgoňa et al. (Drgoňa et al., 2020) and Pinto et al. (Drgoňa et al., 2020), the development of robust data driven or model based controllers critically depends on validated simulation environments that accurately replicate building thermodynamics and system behavior. TRNSYS, with its modular structure and proven effectiveness in geothermal system research, forms an appropriate and defensible choice.

2.5.2. TRNSYS: A Modular Simulation Environment

Having established TRNSYS as a general-purpose engine, this section substantiates that claim by examining how its modular architecture is leveraged in recent, cutting-edge research. Its core strength lies in modeling complex, hybrid systems where multiple technologies interact. A prime example is the detailed simulation of a solar-assisted heat pump coupled with underground thermal storage; a system designed to use surplus solar electricity for heating. In this work, TRNSYS served as the central engine, but its true

flexibility was shown through its co-simulation with MATLAB, which allowed for the development and testing of advanced, inverse-grey-box control models, a task that would be impossible in a more rigid simulation environment (Eze, 2024).

Building on this theme of integration, TRNSYS excels not just in co-simulation but in its ability to act as a central integration hub for models developed in entirely different software. This is critical for long-term performance predictions. For instance, when analyzing the 15-year performance of a GSHP system, a highly detailed ground heat exchanger model was first created and validated in MATLAB, while the building's dynamic load was calculated in TRNBuild. TRNSYS then seamlessly imported these externally-validated sub-models to create a comprehensive system simulation. This capacity to serve as a platform where specialized, best-in-class models can be brought together is a defining feature of a truly general-purpose research tool (Mohammadzadeh Bina et al., 2024). This power extends beyond novel designs to address the critical challenge of retrofitting a representative building. TRNSYS has been used to model the addition of a GSHP to a conventional chiller-boiler system, demonstrating a 50% reduction in energy demand and, crucially, confirming the long-term thermal stability of the ground over a decade (Wang et al., 2024). The platform's adaptability is also proven across diverse geographical contexts, from validating geothermal cooling strategies in the hot, arid climate of Egypt (Fouad et al., 2024) to other complex applications worldwide.

Perhaps the most compelling testament to its credibility is its role as a high-fidelity benchmark against which other models are judged. In a study of a monitored Near-Zero Energy Building, a detailed TRNSYS model was meticulously calibrated with high-resolution data. This calibrated model then served as the "ground truth" to validate a simpler, standardized modeling approach. This demonstrates that TRNSYS is trusted by the research community not just as a simulation tool, but as a reliable benchmark for validating new methods and ensuring accuracy in energy performance analysis (Paola Rocca et al.). Collectively, these applications paint a clear picture: TRNSYS is a comprehensive and

adaptable research environment for modeling, integrating, and most critically validating the performance of complex energy systems.

2.5.3. Justification for Tool Selection

The selection of a simulation tool is a critical methodological decision. The choice of TRNSYS for this study is a deliberate one, rooted in its unique capacity for flexibility, extensibility, and computational performance, attributes essential for advanced research in areas like digital twin development and real-time optimization (Goudarzi et al., 2023).

A primary advantage of TRNSYS is its internal extensibility. Unlike more rigid platforms, its open architecture empowers researchers to develop custom components ('Types') when standard models are insufficient. For instance, to accurately model the complex thermal interactions between geothermal boreholes, a new, more physically rigorous component was developed from fundamental principles and validated against experimental data (Castro-García et al., 2025). This capability to create and integrate bespoke models is not an isolated feature; it is actively leveraged by the research community to overcome common simulation bottlenecks, such as improving the computational efficiency of standard models (De Rosa et al., 2015), enhancing the fidelity of short-term dynamics (Cazorla-Marín et al., 2020), and modeling the irregular geometries common in real-world projects (Kirschstein et al., 2025).

Beyond its internal flexibility, a tool's power is amplified by its ability to interface with external environments for specialized tasks. A comparative study highlighted the superior flexibility of the TRNSYS-MATLAB framework over other common coupling programs like GenOpt. This integration unlocks critical capabilities essential for this research, most notably the ability to perform multi-objective (Pareto) optimizations and leverage powerful commercial solvers, positioning TRNSYS as an ideal platform for advanced control and optimization studies (Meiers & Frey, 2025). This interfacing is not limited to co-simulation;

it also allows TRNSYS to act as an integration hub for pre-calculated results, such as importing detailed thermal loads from other specialized software (X. Wang et al., 2025b).

This flexible, integrated approach stands in sharp contrast to the workflow of other leading engines. While EnergyPlus is highly validated, its extensibility is primarily achieved through co-simulation via middleware (Muslim, 2021). More critically for research involving iterative processes, its computational overhead can become a significant bottleneck. A study using EnergyPlus for multi-objective optimization explicitly identified the “time-consuming” nature of the engine as a major limitation, flagging the search for a more computationally efficient alternative as a key direction for future work (Akraminejad et al., 2025). Therefore, the decision to use TRNSYS is a strategic one, based on its proven ability to couple effectively with powerful external tools (Meiers & Frey, 2025), develop custom internal components to push research boundaries (Castro-García et al., 2025), and crucially, avoid the computational bottlenecks reported for other leading tools in iterative workflows (Akraminejad et al., 2025). This balance makes TRNSYS the most suitable simulation environment for the objectives of this research.

2.6 Review of Previous Studies on Load Analysis and Modeling

Having justified the choice of TRNSYS as the principal simulation engine, attention must shift from the tool itself to the credibility and applicability of the models it generates. A simulation model is an abstract representation of reality; its usefulness depends on a sound anchoring process. This process takes place in three critical, interrelated phases set out in the literature: (1) Calibration and Validation, which bridges the gap between simulated predictions and physical reality; (2) Sensitivity and Uncertainty Analysis, moving the focus from single-point accuracy to risk quantification and parameter influence; and (3) Application in Case Studies, where validated frameworks are put to work for the

optimization of design and operation in specific climatic contexts. The purpose of this section is to review the methodologies associated with these phases critically.

2.6.1. Studies on Model Calibration and Validation

One of the significant challenges in BEM is the so-called "performance gap," defined as the difference between simulated energy consumption and measured operational data. Even though vast amounts of literature are available on methodologies to bridge this gap, recent research underscores that calibration is not merely a statistical exercise; the model's intended purpose must drive it.

A. Automated vs. Manual Methodologies

The literature thus adopts automated, optimization-based calibration for a variety of applications to obtain high-fidelity "Digital Twins" (e.g., fault detection or real-time control). Several investigations using genetic algorithms have shown that it is feasible to reduce deviations from more than 35% in baseline design models to less than 4% in calibrated models while meeting strict hourly benchmarks, such as NMBE and Cv(RMSE), specified by ASHRAE Guideline 14 (Pachano & Bandera, 2021). These generally rely on high-resolution data streams to fine-tune several thousand parameters simultaneously. However, for retrofit analysis or design optimization, manual calibration strategies based on simplified data can be equally effective. Indeed, studies demonstrate that a few dominant parameters, refined by short-term measurements of indoor temperature or CO₂ concentration as a proxy for occupancy, will suffice for models that are robust enough in their prediction of annual energy savings (Tomrukçu et al., 2024), (Tozlu, 2025).

B. The Principle of Equifinality and Calibration Goals

Another key finding of recent studies is the notion of "equifinality" - that there is not one unique best fit, but rather multiple different combinations of parameter inputs can produce the same output error. Cheng et al. (Cheng et al., 2024) see this as evidence that the search

for a single "true" model must give way to a focus on developing a model credible for its intended purpose. In their comparative study, it was found that higher levels of calibration detail improve absolute accuracy but do not affect the ranking of retrofit options. A model for comparative analysis - like the one being developed here - therefore does not require the same level of detailed validation as a model used for model-predictive control.

C. Challenges in Complex Environments

Calibration protocols are further muddled for buildings exhibiting stochastic behaviors. In decentralized systems, or indeed buildings hosting substantial unregulated loads, such as hospitals or hotels, the strict adherence to hourly statistical benchmarks is often misleading, according to (Rotimi et al., 2017) and (da Silva et al., 2021). In such cases, as suggested by the literature, validation should focus on capturing the aggregate system dynamics and thermodynamic trends rather than replicating every stochastic fluctuation caused by occupant behavior.

2.6.2. Studies on Sensitivity Analysis of Building Parameters

Once a model is validated, SA and UA are conducted to determine the most influential performance drivers. It is an essential step beyond deterministic predictions toward a probabilistic understanding of system performance.

A. From Operational to Environmental Scope

Traditionally, SA/UA focused on operational energy parameters, such as setpoints and envelope insulation. However, as decarbonization goals have expanded, the boundary conditions have begun to include environmental impacts. Recent literature has combined SA with LCA to consider the long-term effects of design decisions. Such a change in

boundary conditions often reorders the ranking of essential parameters; for example, when GWP minimization is performed instead of energy use, the embodied carbon of materials and the carbon intensity of the energy source become more crucial than operational variables (Roland et al., 2022). This shows the precise definition of system boundaries (operational vs. life-cycle) before analysis is essential.

B. Handling Second-Order Uncertainty

A critical limitation of the conventional Global Sensitivity Analysis is its dependence on operational assumptions, also known as “second-order uncertainty”. Studies employing Sobol indices have shown that the ranking of design variables, for instance, which is more critical, window SHGC or lighting efficiency, is dynamic and not fixed. It changes with changes in occupant density or temperature setpoints (Young-seo, 2021). Therefore, valid decision-making needs these operational conditions to be treated as uncertain variables themselves, rather than fixed inputs.

C. Computational Barriers and Surrogate Modeling

However, performing extensive SA/UA using physics-based engines such as TRNSYS may require thousands of simulation runs, resulting in an unacceptably high computational burden. Therefore, ML surrogate models have recently become increasingly prominent in the area. The surrogates approximate the complex simulation; they are trained on a smaller dataset of simulation results and validated against the complete model using metrics such as the coefficient of determination (R^2). After validation, these lightweight models enable researchers to perform extensive uncertainty quantification and risk assessment in near real time (Tian, 2024), making probabilistic analysis feasible for complex integrated systems.

2.6.3. Case Studies of Commercial/Institutional Buildings in Cold Climates

The methodologies of calibration and analysis find their practical application in case studies. To understand the state of the art in cold climates, this review categorizes recent studies into a three-level hierarchy: component optimization, system integration, and holistic implementation.

Level 1: Component-Level Optimization

At the fundamental level, research focuses on optimizing individual passive elements to reduce thermal loads. For example, parametric studies in cold regions have identified high-performance curtain wall systems as a critical intervention, capable of reducing energy demand by up to 69.7% when optimized for specific orientation and solar gain targets (Liu et al., 2024). These studies confirm that minimizing the passive load is a prerequisite for the efficient operation of active systems.

Level 2: Active System Integration and Form

Moving to the system level, the focus shifts to the interaction between building form and energy generation. Research demonstrates that compact building massing is essential in cold climates to minimize heat loss and improve the efficiency of active systems (Guo et al., 2025). More importantly, the integration of renewable generation with heating systems is a key area of innovation. Case studies analyzing hybrid configurations—such as Ground Source Heat Pumps (GSHP) coupled with PV or district heating—have shown that these integrated systems offer the most cost-optimal pathway for decarbonization, significantly outperforming standalone envelope upgrades in terms of Life Cycle Cost (LCC) (Hu, 2025).

Level 3: Market Realities and Implementation Barriers

Finally, the literature contrasts these technical optimizations with market realities. While academic studies often prioritize maximum thermodynamic efficiency or lowest LCC, empirical research on office retrofits in Finland reveals that decision-making is often driven by risk aversion and initial capital constraints (Marttila, 2025). This suggests that for a

proposed solution (like the geothermal integration explored in this thesis) to be viable, it must be technically robust and effectively sized to balance performance with complexity—a gap that this thesis aims to address through accurate simulation and sizing

2.7 Identifying the Research Gap and Objectives

In this work, a representative office building is used as a reference model to develop and validate the simulation methodology. The above literature review uncovers an important paradox in the field of building energy modeling. The community possesses, on one hand, exceptionally sophisticated tools such as TRNSYS, proven methodologies for model calibration (Pachano & Bandera, 2021), (Tomrukçu et al., 2024), and powerful analytical techniques for finding optimal, system-level decarbonization pathways (Liu et al., 2024), (Hu, 2025). On the other hand, a stark disconnect exists between those technically optimal solutions and pragmatic, risk-averse decisions in the real world (Marttila, 2025). The implication of this synthesis is that a core barrier to implementing deep, sustainable retrofits is not an absence of advanced optimization strategies but rather an absence of confidence in the foundational models upon which those strategies are built.

This points to a fundamental research gap in that while there have been myriad studies relating to the simulation and optimization of particular energy systems-e.g., HVAC and renewables-they almost invariably assume the availability of a dependable and validated building load model. The literature shows that the elaboration of this essential "digital twin" is thus both a challenging and sensitive process to uncertain inputs, like internal gains and infiltration (Rotimi et al., 2017), (da Silva et al., 2021). Yet, the rigorous process of developing, simulating, and critically analyzing the thermal loads of a complex institutional building-let alone applying an energy system solution to it-is the initial, critical step that is so often skipped or simplified. This paper counters that such a step is not preliminary, but rather paramount. It represents the non-negotiable precursor to any credible subsequent

analysis, and its absence is a primary source of the very investment risk that stifles innovation.

To address this foundational gap, this thesis will pivot away from the simulation of a specific HVAC system and instead concentrate on the rigorous and transparent process of establishing a credible baseline energy model for the research facility. The main objectives which form the roadmap in this research are:

1. To Develop a High-Fidelity Model: Create in TRNSYS a detailed, multi-zone dynamic thermal model of the building by accurately characterizing envelope, internal mass, and operational parameters from architectural documents and engineering standards.
2. Foundational Loads Simulation: Accurately simulate the hourly and annual heating and cooling loads, with a pure focus on the quantification of the intrinsic thermal demand of the building dictated by its physics and climate, in complete independence from any energy supply system.
3. Validation and Critical Analysis: These include the validation of the simulated demand against measured data and, importantly, the investigation into sources of any performance gap. This goes beyond simple calibration to provide critical insights into assumptions relating to infiltration, ventilation, and internal gains.
4. Digital Baseline: Provide a valid, transparent, and highly documented thermal load model that can be used as a trusted basis for further research; facility managers, engineers, and researchers will be able to study retrofits and new energy technologies with confidence.

By focusing on this critical first step, the present study provides not just a model of a single building but a clear, replicable methodology for reducing uncertainty and building confidence to bridge the gap between simulation and real-world implementation.

3 Research Method

The heating and cooling loads of the building are calculated based on a transient energy balance applied to each thermal zone. This approach allows the required HVAC system capacity and dynamic thermal behavior of the building to be determined. The simulations are performed in TRNSYS, where each thermal zone is modeled using a lumped-capacitance method. In this approach, the indoor air, building envelope, roof, and fenestration are treated as a single thermal mass with a uniform temperature, and spatial temperature gradients within the zone are neglected. In this approach, U represents the overall heat transfer coefficient, and the capacitance is also overall. In other words, the whole zone behaves like a single thermal mass exposed to the outdoor temperature.

The primary boundary condition applied to the thermal zone is the ambient outdoor temperature, which drives heat transfer through the building envelope. Ventilation and infiltration airflows introduce additional heat exchange between the zone and the outdoor environment. Internal heat gains from occupants, lighting, and equipment are also included. Boundary condition will be defined in following section when explaining how to fill different parts of the TRNSYS. In TRNSYS, the thermal loads are evaluated using the

following primary governing equation:

$$\frac{dT}{dt} = \frac{UA}{cap} (T_{amb} - T) + \frac{\dot{m}_{vent} Cp_{air}}{cap} (T_{vent} - T) + \frac{\dot{m}_{inf} Cp_{air}}{cap} (T_{inf} - T) + \frac{\sum Q_{gains}}{cap} \quad (5)$$

$$\dot{Q}_{inf} = \dot{m}_{inf} Cp_{air} (T_{inf} - T) \quad (6)$$

$$\dot{Q}_{vent} = \dot{m}_{vent} Cp_{air} (T_{vent} - T) \quad (7)$$

$$\sum Q_{gains} = Q_{lights} + Q_{equip} + Q_{people} \quad (8)$$

U building loss coefficient(kJ/hr-m²-C)

Cap building capacitance (kJ/C)

$C_{p_{air}}$	specific heat of building air (kJ/kg-C)
ρ_{air}	density of building air (kg/m ³)
T_{vent}	temperature of ventilation air (C)
m_{vent}	ventilation air mass flow rate (kg/hr)
T_{amb}	ambient temperature (C)
m_{inf}	mass flow rate of infiltration air
Q_{lights}	rate of energy gain from lights (kJ/hr)
Q_{equip}	rate of energy gain from equipment (kJ/hr)
Q_{peop}	rate of sensible energy gain from people (kJ/hr)
T_{zone}	zone temperature (C)
Q_{infls}	sensible energy gain from infiltration (kJ/hr)
Q_{vents}	sensible energy gain from ventilation (kJ/hr)

The left-hand side of the equation represents the rate of change of internal energy, whereas the right-hand side accounts for heat transfer through the building envelope, as well as ventilation, infiltration, and internal heat gains. Heat transfer through the envelope is discussed in Section 2.1, internal gains in Section 2.2, infiltration in Section 2.4, and ventilation in Section 2.5.

After determining the total thermal load, it is desirable to modify the model control strategy to a temperature-based control scheme. For each thermal zone, the heating and cooling functions must be deactivated in order to transition the control system from an energy-based approach to a temperature-based one.

3.1 Building Energy Model Development

The initial stage of the simulation process involves developing a three-dimensional model of the building in SketchUp using the TRNSYS3D plug-in. Although realistic construction data are used, the modeled building serves as a representative reference building rather than a specific monitored facility. Particular emphasis is placed on accurately representing the office building geometry and correctly classifying construction elements (such as walls and ceilings) as either external surfaces or internal/adjacent components. After the modeling phase is completed, the TRNSYS3D model is imported into the TRNSYS simulation environment. Figure 4 presents a perspective view of the building.

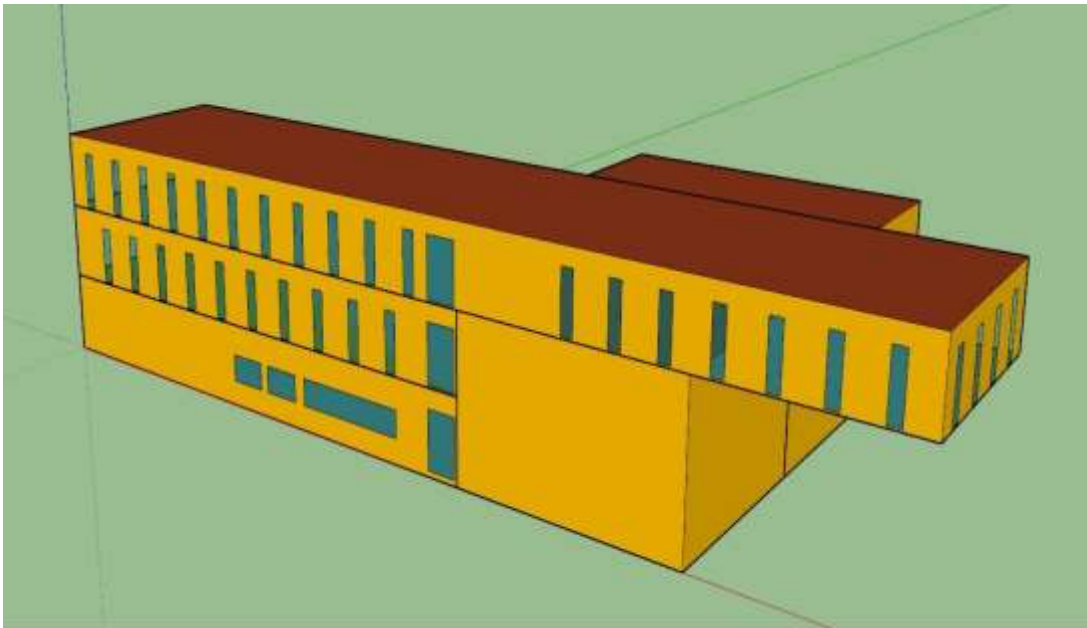


Figure 4. SketchUp model of the Building with help of TRNSYS3D

There are several methods for importing a TRNSYS3D model into TRNSYS; in this project, three approaches were employed. To import the *Building.idf* file, the Type 56 component

was utilized. In addition, defining the building's geographical location is essential; in this study, the building is located in the Northern Hemisphere.



Figure 5. Importing TRNSYS3D file into TRNBuild

After that, by right-clicking on component Type 56 and selecting "Edit Building", a separate software called TRNBuild opens.

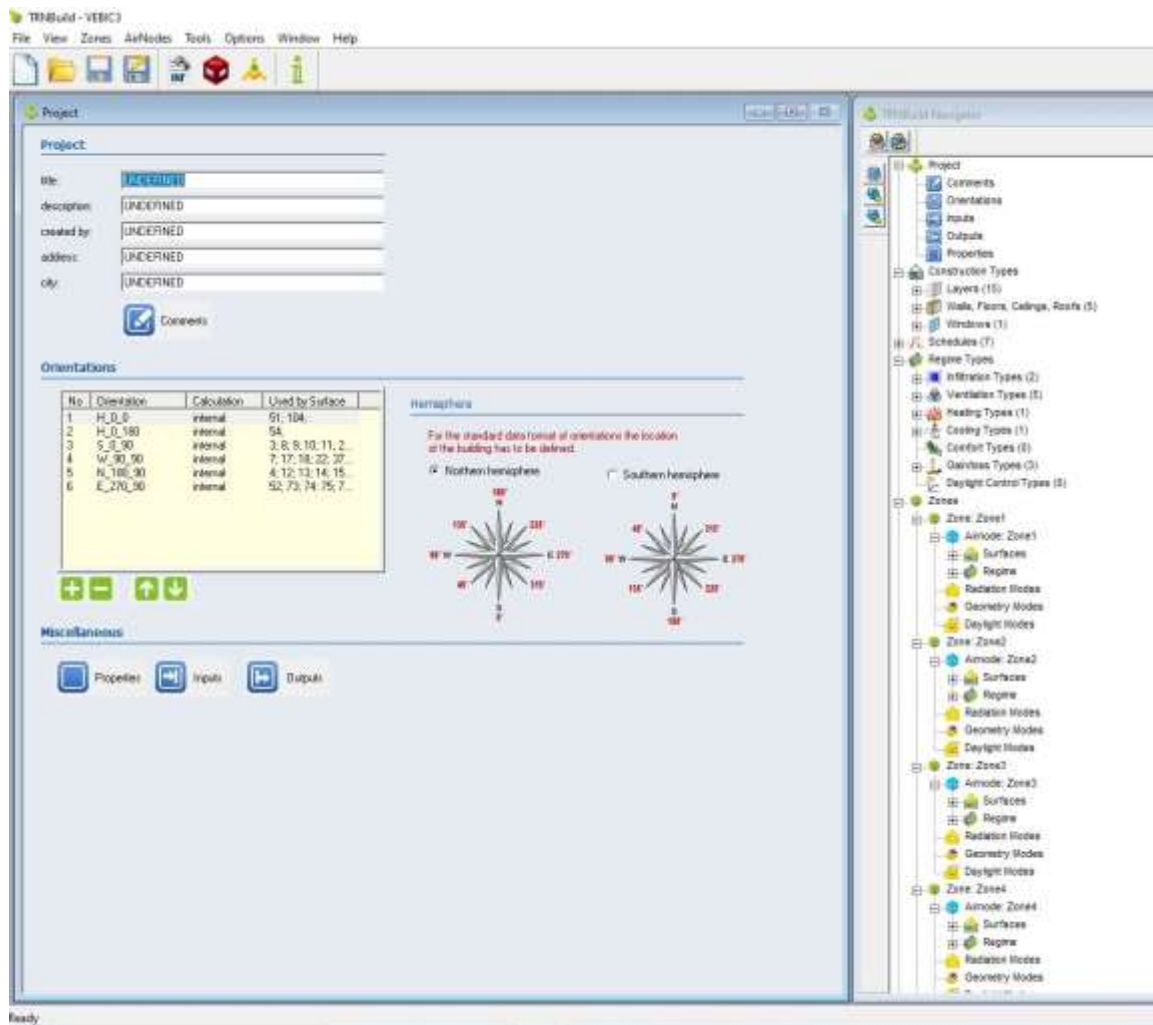


Figure 6. TRNBuild simulation Environment

In TRNBuild, characteristics such as wall and window materials, infiltration rate, ventilation, and internal gains from lights, people, and equipment can be defined.

First, the materials of the external wall were defined as shown in the table to obtain the total U-value of the wall, with the data based on real conditions.

Table 1. Material of external walls

Layer	k (kJ/h·m·K)	cp (kJ/kg·K)	Density (kg/m ³)	Thickness (m)	R = L/k (m ² ·K/W)
Gypsum Board	0.90	1.09	950	0.0125	0.05
Concrete	6.12	0.88	2300	0.10	0.059
Air Gap	0.0417	—	—	0.02	0.11
Insulation	0.126	0.80	40	0.20	5.71
Brick	2.16	0.84	1800	0.10	0.167

Construction Type Manager

"Construction Type" Manager

construction type: EXT_WALL

Layer

front / inside

No.	Layer	Thickness	Type
1	GypBoard	0.013	massive
2	Concrete	0.100	massive
3	AirGap		massless
4	Insulation	0.200	massive
5	Bricks	0.100	massive

back

total thickness: 0.413 m

u - value: 0.158 W/m² K for reference only
(incl. h_i=7.7 W/m² K and h_o=25 W/m² K)

Solar Absorptance

front: 0.4

back: 0.5

Longwave Emission Coefficient

front: 0.9

back: 0.9

Note:
The emissivity of inside surfaces are applied by the detailed longwave radiation mode only!
For the standard model fixed values of 0.9 are used.

Convective Heat Transfer Coefficient

front

userdefined internal calculation

floor ceiling vertical wall

back

userdefined internal calculation

|: 1*HOUTSIDE kJ/h m² K

Figure 7. Layers and Materials of the external walls

The materials of the roof were defined as shown below to obtain the total U-value of the roof, based on real conditions.

Table 2. Material of external roofs

Layer	k (kJ/h·m·K)	cp (kJ/kg·K)	Density (kg/m ³)	Thickness (m)	R = L/k (m ² ·K/W)
Gypsum Board	0.90	1.09	950	0.0125	0.05
Concrete	6.12	0.88	2300	0.10	0.059
Air Gap	0.65	—	—	0.02	0.11
Insulation	0.126	0.80	40	0.30	8.57
Wooden	0.504	1.60	500	0.02	0.04
Bitumen	0.612	1	1200	0.005	0.008

Construction Type Manager

"Construction Type" Manager ✓ ✕

construction type:

Layer

front / inside

No.	Layer	Thickness	Type
1	GypBoard	0.013	massive
2	Concrete	0.100	massive
3	AirGap		massless
4	Insulation	0.350	massive
5	Wood	0.100	massive
6	Bitumen	0.010	massive

back

total thickness: m

u - value: W/m² K for reference only
(incl. h_i=7.7 W/m² K and h_o=25 W/m² K)

Solar Absorptance

front: -

back: -

Longwave Emission Coefficient

front: -

back: -

Note:
The emissivity of inside surfaces are applied by the detailed longwave radiation mode only!
For the standard model fixed values of 0.9 are used.

Convective Heat Transfer Coefficient

front

userdefined internal calculation

floor ceiling vertical wall

back

userdefined internal calculation

kJ/h m² K

Figure 8. Layers and Materials of the external roofs

The figure 8 shows the convective heat transfer coefficient front has internal calculation and for back is an input set as HOUTSIDE.

Table 3. Material of external the ground floor

Layer	k (kJ/h·m·K)	cp (kJ/kg·K)	Density (kg/m ³)	Thickness(m)	R = L/k (m ² ·K/W)
Concrete	6.12	0.88	2300	0.10	0.059
Plastic	1.80	2.0	920	0.001	0.002
Insulation	0.126	1.40	25–40	0.20	5.71
Sand/Gravel	3.60	0.80	1800	0.20	0.056
Soil	2.88	0.80	1600		

Construction Type Manager

"Construction Type" Manager

construction type:

Layer

front / inside

No.	Layer	Thickness	Type
1	Concrete	0.100	massive
2	Plastic	0.010	massive
3	Insulation	0.185	massive
4	Gravel	0.200	massive
5	Soil	0.200	massive

back

total thickness: m

u - value: W/m² K for reference only
(incl. h_i=7.7 W/m² K and h_o=25 W/m² K)

Solar Absorptance

front: -

back: -

Longwave Emission Coefficient

front: -

back: -

Note:
The emissivity of inside surfaces are applied by the detailed longwave radiation mode only!
For the standard model fixed values of 0.9 are used.

Convective Heat Transfer Coefficient

front

userdefined internal calculation

floor ceiling vertical wall

back

userdefined internal calculation

kJ/h m² K

Figure 9. Layers and Materials of the external the ground floor

For the adjacent wall, the combination of wall materials is shown in Figure 10.

Construction Type Manager

"Construction Type" Manager ✓ ✕

construction type:

Layer

front / inside

No.	Layer	Thickness	Type
1	GypBoard	0.013	massive
2	MIWD	0.100	massive
3	GypBoard	0.013	massive

back

total thickness: m

u - value: W/m² K *for reference only*
(incl. h_i=7.7 W/m² K and h_o=25 W/m² K)

Solar Absorptance

front: -

back: -

Longwave Emission Coefficient

front: -

back: -

*Note.
The emissivity of inside surfaces are applied by the detailed longwave radiation mode only!
For the standard model fixed values of 0.9 are used.*

Convective Heat Transfer Coefficient

front

userdefined internal calculation

floor ceiling vertical wall

back

userdefined internal calculation

floor ceiling vertical wall

Figure 10. Layers and Materials of the external adjacent walls

The most important factors for windows are the U-value and G-value. Based on the building documentation, the building's U-value and G-value are 1 and 0.5, respectively.

The screenshot shows the 'Window Type Manager' interface with the following parameters:

- Window Type:** EXT_WINDOW1
- Glazing:**
 - ID number: 14205
 - u-value: 1.01 W/m²K
 - g-value: 0.5 %/100
 - ID spacer: 4 Insulated
- Frame:**
 - Window frame fraction: 11.15
 - τ-value (1/R): 11.17
 - solar absorption: 0.6
 - emissivity: 0.9
- Optional Properties of Shading Devices:**
 - Additional Thermal Resistance: internal device (0), external device (0)
 - Reflection Coefficient of Internal Device: towards window (0.5), towards zone (0.5)
 - Emittance of Internal Device towards zone: 0.9
 - Fraction of abs. solar radiation of internal device transformed to a conv. heat flow rate (CCSHDR): 0.5
 - Add to conv. gain to mode: 0
- Daylight Properties:**
 - Visible light transmittance: 0.72
 - Material name unshaded: undefined
 - Material name shaded: undefined
- Glazing + Frame:**
 - Front (inside) - Convective Heat Transfer Coefficient: 11
 - Rear (outside) - Convective Heat Transfer Coefficient: 17
 - Excluded Energy: total renewable primary energy (0 MJ/m²), total nonrenewable primary energy (0 MJ/m²)

Figure 11. Layers and Materials of the external windows

To reduce model complexity and avoid redundant parameters, all default layers, walls, and windows that were not utilized in the building model were removed from TRNBuild. Only the construction elements explicitly defined for the case-study building were retained for the simulations. After completing this cleanup, the TRNBuild file was saved, and the corresponding building variables in the Type 56 component were updated to ensure consistency between the building definition and the simulation environment.

After completing the physical characteristics of the building, the next step is to consider the driving forces, the most important of which are in the weather component. In this simulation, the TMY3 format has been used. Variables such as TAMB, RELHUMAMB, TSKY, TSGRD, AZEN, GRDREF, and TGROUND can be connected directly to the weather data, while for AAZM, an orientation equation must be defined.

There is an empirical equation by McAdams that describes the relationship between convective heat transfer coefficient (H) and wind speed:

$$h_{\text{external}} = 3.8 \text{ Wind speed} + 7.4 \quad [h_{\text{ext}}: \text{Wm}^{-2}\text{K}^{-1}, V_{\text{wind}}: \text{ms}^{-1}] \quad (9)$$

Since the external convective heat transfer coefficient h_{external} must be specified as an input for both walls and windows, the following equation is applied. To implement this relationship, a new equation component is created in which the wind speed—obtained from the weather data component—is defined as the independent variable, while h_{external} is specified as the dependent variable.

3.2 Internal Gains

Another significant driving factor in building energy performance is internal heat gains, which originate from lighting, equipment, and occupants. These gains vary over time and are therefore non-uniform across daily and weekly periods. As a result, they must be defined using time-dependent schedules rather than as constant values. In the simulation, such schedules are implemented through component Type 14.

To define internal gains, the user must right-click on component Type 56 and select “Edit Building” to open the TRNBuild interface. Within TRNBuild, the Gains/Losses section is accessed by right-clicking and selecting “Add Gain from Library” to introduce a new occupant-related gain. From the available library options, the ASHRAE_130W-Person gain

type is selected to represent heat gains from occupants.

Gain Library

"Gains"

Program Library User Library

Program Library 18.06.0001;

C:\TRNSYS18\Building\Lib\American\tnbuild_gain.lib

No.	Name	Description	Category	Absolute / area-related	Convective Power [kJ/hr]	Radiative Power [kJ/hr]	Electric Power Fraction [-]	Humidity [kg/hr]
1	ASHRAE_95W-Person_A...	Degree of activity I (seated...	people	absolute	93.6	140.4	0	0.044
2	ASHRAE_105W-Person_A...	Degree of activity II (seate...	people	absolute	100.8	151.2	0	0.052
3	ASHRAE_115W-Person_A...	Degree of activity III (seate...	people	absolute	100.8	151.2	0	0.066
4	ASHRAE_130W-Person_A...	Degree of activity IV (mode...	people	absolute	113.4	156.6	0	0.081
5	ASHRAE_145W-Person_A...	Degree of activity VI (walki...	people	absolute	113.4	156.6	0	0.103
6	ASHRAE_160W-Person_A...	Degree of activity VII (sede...	people	absolute	120.96	167.04	0	0.118
7	ASHRAE_220W-Person_A...	Degree of activity VIII (light...	people	absolute	146.88	141.12	0	0.206
8	ASHRAE_250W-Person_A...	Degree of activity IX (mode...	people	absolute	165.24	158.76	0	0.236
9	ASHRAE_295W-Person_A...	Degree of activity X (walkin...	people	absolute	201.96	194.04	0	0.272
10	ASHRAE_425W-Person_A...	Degree of activity XI (bowli...	people	absolute	281.52	330.48	0	0.375
11	ASHRAE_425W-Person_A...	Degree of activity XII (heav...	people	absolute	281.52	330.48	0	0.375
12	ASHRAE_470W-Person A...	Deegree of activty XIII (hea...	people	absolute	306.36	359.64	0	0.42

Selected Types

No.	Name	Description	Category	Absolute / area-related	Convective Power [kJ/hr]	Radiative Power [kJ/hr]	Electric Power Fraction [-]	Humidity [kg/hr]
1	ASHRAE_130W-Person_A...	Degree of activity V (standi...	people	absolute	113.4	156.6	0	0.081

Figure 12. Adding people's gain from the program library
Similarly, the gains from lights and equipment are defined as shown.

Gain/loss Type Manager

"Gain/loss Type" Manager ✓ ✕

Gain/loss type name: LIGHT

Gain/loss Category

lights

absolute gain/loss gain/loss related to reference floor area

Radiative

▶ 0.8 kJ / h

Convective

▶ 0.2 kJ / h

Electric Power Fraction

fraction of actual radiative + convective power

▶ 0 -

Note: The electric power has no influence on the thermal energy balance.

Abs. Humidity

▶ 0 kg / hr

Figure 13. Definition of lighting gain

Then, these gains must be allocated to the five different zones of the building in TRNBuild. For this purpose, we define Peo_Z1 to Peo_Z5, Eqp_Z1 to Eqp_Z5, and Light_Z1 to Light_Z5.

It is possible to define maximum gains based on the floor area (density). Recommended values are approximately 10.8 W/m² for lighting, 21.5 W/m² for equipment, and 1 person per 21 m² for occupancy. Since gains must be defined based on area, it is convenient to create variables for the areas of the different zones. Because TRNSYS uses kJ/h as the energy unit, the gains should be multiplied by 3.6. As a result:

$$\text{LightDen} = 10.8 \cdot 3.6; \text{EqpDen} = 21.5 \cdot 3.6, \text{ and } \text{OccDen} = 1/21. \quad (8)$$

For fraction data, the graph below can be inserted into component Type 14. These values are taken from ASHRAE 90.1-2007.

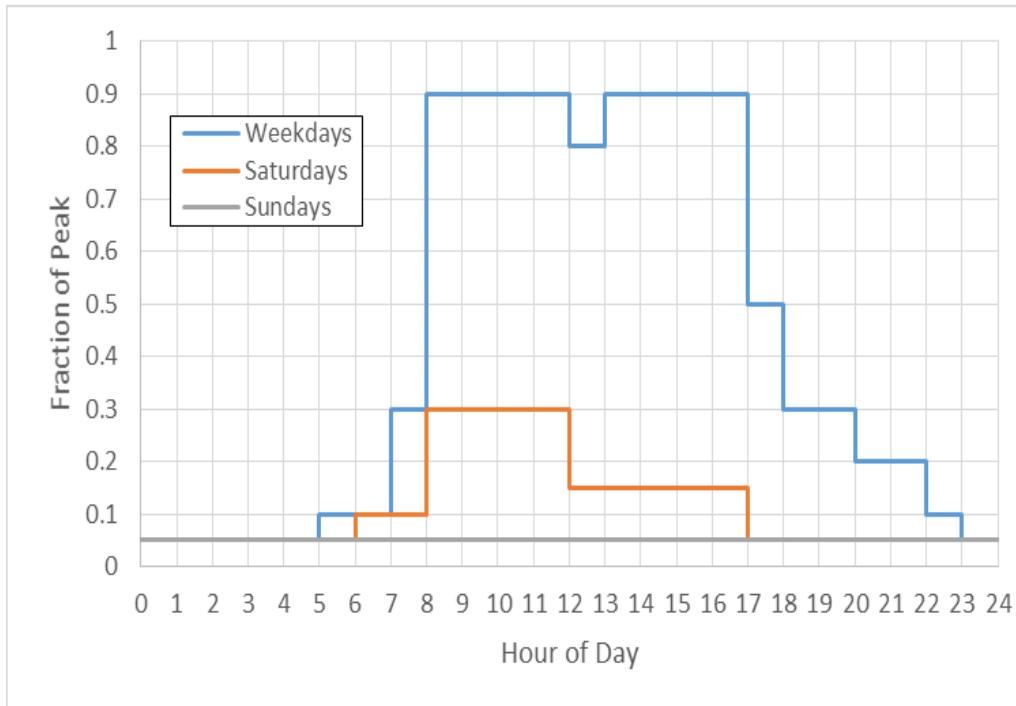


Figure 14. Lighting and Equipment Gain Schedules (TRNSYS, 2024)

To make it clearer, the details are shown in the table below:

Table 4. Equation of gains

Zone	Square m ²	Q_{People}	Q_{Lights}	$Q_{\text{Equipment}}$
1	458.395	FracOcc*OccDen*zone1	FracLE*LgtDen*zone1	FracLE*EqpDen*zone1
2	458.395	FracOcc*OccDen*zone2	FracLE*LgtDen*zone2	FracLE*EqpDen*zone2
3	814.167	FracOcc*OccDen*zone3	FracLE*LgtDen*zone3	FracLE*EqpDen*zone3
4	192.9	FracOcc*OccDen*zone4	FracLE*LgtDen*zone4	FracLE*EqpDen*zone4
5	501.6	FracOcc*OccDen*zone5	FracLE*LgtDen*zone5	FracLE*EqpDen*zone5

With these definitions and formulas, the internal gains are clearly determined and should be connected to the inputs previously defined in TRNBuild. In this way, all internal gains are addressed in the simulation.

3.3 Internal Capacitance:

The definition of capacitance is: $\text{Capacitance} = mc_p$

Since the building is not empty and always contains equipment, devices, and furniture, it is not accurate to simply multiply the building volume by the air density and then by the specific heat capacity of air. The additional items mentioned above affect the temperature response rate. Therefore, they should be considered, and an estimation can be made that more closely reflects reality by multiplying the air capacitance by a factor of five. According to the TRNSYS documentation:

“There are many things inside the zone (furniture, furnishings, internal walls, etc.) that add to the capacitance and slow the zone’s response to temperature changes. Leaving the zone at the default capacitance will over-predict how quickly the zone temperature will change. There is no definitive rule for adjusting the capacity of the zone, but typically we will multiply the air-only capacity by 5 to 15 times.”

In this project, we adopt this assumption and multiply the capacitance of all zones by 5. The table below shows the default TRNSYS calculations and their values after applying this multiplication factor.

Table 5. Capacitance of zones

Zones	Capacitance of the air inside empty zones	Capacitances considering equipment
Zone1	2365.32 KJ/K	11826.6 KJ/K
Zone2	2200.3 KJ/K	11001.5 KJ/K
Zone3	3908 KJ/K	19540 KJ/K
Zone4	1921.28 KJ/K	9606.4 KJ/K
Zone5	5477.47 KJ/K	27387.3 KJ/K

The moisture capacitance can also be adjusted by increasing it tenfold, similar to the thermal capacitance.

3.4 Infiltration

The infiltration rate is approximately $5.4 \text{ m}^3/\text{h}\cdot\text{m}^2$ of external wall area, based on ASHRAE HOF, Chapter 16.

$$\text{ACH} = (\text{Infiltration rate} \times \text{External wall area}) / \text{Volume}$$

Table 6. Infiltration rate

Zone No.	Wall Area	Volume	ACH
1	153.27+119.73+55.3	1971	0.9
2	142.58+51.44+111.38	1833.58	0.9
3	2*51.44+2*253.24	3252.67	1
4	51.44+124.5	1601	0.6
5	207.48+200.2+200.2+18	4564.56	0.74

Four different infiltration rates are defined for the five zones and allocated accordingly to each zone.

3.5 Ventilation Air




It is essential to provide fresh air for occupants of buildings. In many cases, the outside air must be treated before it can be used indoors. As mentioned in Equation (1-1), determining the ventilation air load is necessary to calculate the total building load.

According to ASHRAE Standard 62.1-2004, $0.304 \text{ L/s}\cdot\text{m}^2$ (0.06 cfm/ft^2) and 2.36 L/s per occupant (5 cfm/occupant) of fresh air should be provided whenever the building is occupied.

Again, TRNBuild is used to add inputs for ventilation air. By right-clicking on “Ventilation Types” and selecting “Add Ventilation”, a new ventilation type can be defined. For each zone, a separate ventilation type is created as Vent_Zi ($i = 1$ to 5).

Each ventilation type has three parameters: mass flow rate, temperature, and relative humidity ratio. These are defined respectively as VFLOW_Z1 to Z5, TVENT_Z1 to Z5, and RHVENT_Z1 to Z5.

Ventilation Type Manager

 "Ventilation Type" Manager  

ventilation type:

Supply air flow

mass flow rate kg/h

Specific fan power (related to supply air flow): kJ/hr / (m³/hr)

Note: The spec. fan power has no influence on the thermal energy balance.

Supply air conditioning

external by other component
 internal calculation

Temperature of supply air flow

outside air
 userdefined °C

Humidity of Air Flow

relative humidity
 absolute humidity

outside air
 userdefined %

Figure 15. Adding ventilation types

These inputs are very useful because they are not only used in the calculation of the total load but also connected to the HVAC system after the load calculation. In the final step, the created ventilation types should be allocated to each zone.

Since the inputs VFLOW, TVENT, and RHVENT are defined in TRNBuild, an equation must be created to supply values for them. As mentioned earlier, the fresh air rate is defined based on ASHRAE Standard:

$$\text{Fresh rate} = 0.304 * \text{Zone area} + 2.36 * \text{OccDen} * \text{Zone Area} \quad (10)$$

The ZoneArea and Occupancy Density (OccDen) were already defined earlier for internal gains, so they can be reused here.

TRNSYS provides various functions to simplify equation definitions. One of them is GT, which returns 1 when the fraction of occupancy is greater than zero and 0 when there are no occupants. Using this function, the ventilation volume flow can be defined as:

$$V = \text{GT}(\text{FracOcc}, 0) * (0.304 * \text{Zone area} + 2.36 * \text{OccDen} * \text{Zone Area}) \quad (11)$$

Since the unit is in L/s, a conversion is required to obtain kg/h:

$$\dot{m} = (1.2 * 3600 / 1000) \text{GT}(\text{FracOcc}, 0) * (0.304 * \text{Zone area} + 2.36 * \text{OccDen} * \text{Zone Area}) \quad (12)$$

The table 7 presents the equation definitions for each zone.

Table 7. HVAC settings

Zone No.	Ventilation	
Zone1	VENT_Z1	$\text{gt}(\text{Occ}, 0) * (0.304 * \text{zone1} + 2.36 * \text{OccDen} * \text{zone1}) * (1.2 * 3600 / 1000)$
Zone2	VENT_Z2	$\text{gt}(\text{Occ}, 0) * (0.304 * \text{zone2} + 2.36 * \text{OccDen} * \text{zone2}) * (1.2 * 3600 / 1000)$
Zone3	VENT_Z3	$\text{gt}(\text{Occ}, 0) * (0.304 * \text{zone3} + 2.36 * \text{OccDen} * \text{zone3}) * (1.2 * 3600 / 1000)$
Zone4	VENT_Z4	$\text{gt}(\text{Occ}, 0) * (0.304 * \text{zone4} + 2.36 * \text{OccDen} * \text{zone4}) * (1.2 * 3600 / 1000)$
Zone5	VENT_Z5	$\text{gt}(\text{Occ}, 0) * (0.304 * \text{zone5} + 2.36 * \text{OccDen} * \text{zone5}) * (1.2 * 3600 / 1000)$

Now, it is possible to connect these equations to component Type 56 and link Vent_Zi to VFLOW_Zi. At this stage, since there is no HVAC system yet, TVENT_Z1 to Z5 and RHVENT_Z1 to Z5 can be connected directly to the weather component.

3.6 Heating and Cooling Load

The heating and cooling loads must be defined in TRNBuild. The new heating type is named HEATING, and the setpoint temperature of the zones is defined as THEAT as an input. The sensible heating power should be verified to ensure it always compensates for the full load of the building as needed.

Heating Type Manager

"Heating Type" Manager

heating type: HEATING

Room Temperature Control

set temperature: 1*THEAT °C

Sensible heating power

unlimited
 limited

radiative fraction: 0 -

Electric Power Fraction

fraction of actual sensible power:
 0 -

Note: The electric power has no influence on the thermal energy balance.




Humidification

off
 on

Figure 16. Definition of heating load


Likewise, a cooling type is added to determine the cooling load. The new cooling type is named COOLING, and the setpoint temperature of the zones is defined as TCOOL as an input. The sensible cooling power should be verified to ensure it always compensates for the full load of the building as needed.

Cooling Type Manager

 **"Cooling Type" Manager**  

cooling type:


Room Temperature Control

set temperature:  °C

Sensible cooling power

unlimited
 limited

Electric Power Fraction

fraction of actual sensible power:
 .

Note: The electric power has no influence on the thermal energy balance.

Dehumidification

off
 on

Figure 17. Definition of heating load

After cooling and heating have been activated for each zone, it is time to define the THEAT and TCOOL setpoints. Since these setpoints differ depending on whether the building is occupied or not, the previously defined GT function for occupancy can be used. As GT(Occ, 0) was already established earlier, it can also be applied to define these setpoints.

$$\text{THEAT} = 18.33 + 1.67 * \text{GT}(\text{Occ}, 0) \quad (13)$$

$$\text{TCOOL} = 23.89 - 1.67 * \text{GT}(\text{Occ}, 0) \quad (14)$$

Table 8. Heating & Cooling Loads

	KJ	KJ	KJ	KJ	KJ	KJ	KJ	KJ	KJ	KJ
Period	Q_Heat_Z	Q_Heat_Z2	Q_Heat_Z3	Q_Heat_Z4	Q_Heat_Z5	Q_Cool_Z1	Q_Cool_Z2	Q_Cool_Z3	Q_Cool_Z4	Q_Cool_Z5
8760	2.045E+08	1.19E+08	2.38E+08	1.59E+08	5.00E+08	1.35E+07	2.61E+07	4.15E+07	1.35E+06	1.97E+06
Maximum Instantaneous Values										
	KJ	KJ	KJ	KJ	KJ	KJ	KJ	KJ	KJ	KJ
Maximum	1.32E+05	9.00E+04	1.70E+05	7.69E+04	2.24E+05	6.03E+04	6.30E+04	1.08E+05	2.05E+04	4.66E+04
Time of	2.86E+02	2.88E+02	2.88E+02	2.88E+02	2.88E+02	4.38E+03	4.38E+03	4.38E+03	4.38E+03	4.38E+03
Minimum Instantaneous Values										
	KJ	KJ	KJ	KJ	KJ	KJ	KJ	KJ	KJ	KJ
Minimum	0.00E+00	0.00E+00	0.00E+00	0.00E+00	0.00E+00	0.00E+00	0.00E+00	0.00E+00	0.00E+00	0.00E+00
Time of	7.67E+03	8.51E+03	8.51E+03	7.02E+03	7.00E+03	8.76E+03	8.76E+03	8.76E+03	8.76E+03	8.76E+03
Maximum Integrated Values										
	KJ	KJ	KJ	KJ	KJ	KJ	KJ	KJ	KJ	KJ
Maximum	2.04E+08	1.19E+08	2.38E+08	1.59E+08	5.00E+08	1.35E+07	2.61E+07	4.15E+07	1.35E+06	1.97E+06
Time of	8.76E+03	8.76E+03	8.76E+03	8.76E+03	8.76E+03	8.76E+03	8.76E+03	8.76E+03	8.76E+03	8.76E+03
Minimum Integrated Values										
	KJ	KJ	KJ	KJ	KJ	KJ	KJ	KJ	KJ	KJ
Minimum	2.04E+08	1.19E+08	2.38E+08	1.59E+08	5.00E+08	1.35E+07	2.61E+07	4.15E+07	1.35E+06	1.97E+06
Time of	8.76E+03	8.76E+03	8.76E+03	8.76E+03	8.76E+03	8.76E+03	8.76E+03	8.76E+03	8.76E+03	8.76E+03
Sum (note: sums are set to zero for inputs that were not integrated.)										
	KJ	KJ	KJ	KJ	KJ	KJ	KJ	KJ	KJ	KJ
Total	2.04E+08	1.19E+08	2.38E+08	1.59E+08	5.00E+08	1.35E+07	2.61E+07	4.15E+07	1.35E+06	1.97E+06

However, these setpoints may introduce complications during load determination. Because the power capacities of the heating and cooling components are set to very high values, they respond sharply to variations in the setpoints, resulting in pronounced fluctuations. To mitigate this behavior, it is recommended to add an exclamation mark to the equations above, thereby converting them into fixed numerical values. When the exclamation mark is applied, the remaining elements of the expressions are interpreted as text and are excluded from the calculations.

Subsequently, by running the simulation over a full annual period of 8,760 hours, the maximum loads for each zone can be determined.

With the maximum loads determined for all zones, an appropriate water-source heat pump can be selected for both cooling and heating applications. It should be noted that the cooling load is the primary criterion in heat pump selection, as any shortfall in heating capacity can be compensated through auxiliary heating. All reported values correspond to sensible loads, which must be considered in the heat pump selection process.

The heat pump component requires a performance map, which must be defined for the specific unit being modeled. In this study, the default water-source heat pump available in TRNSYS is employed.

Several input variables are required for the heat pump model. The first two inputs (the dry-bulb temperature and relative humidity) are provided by the building component. The remaining inputs are obtained from the weather component, as illustrated in the figure below.

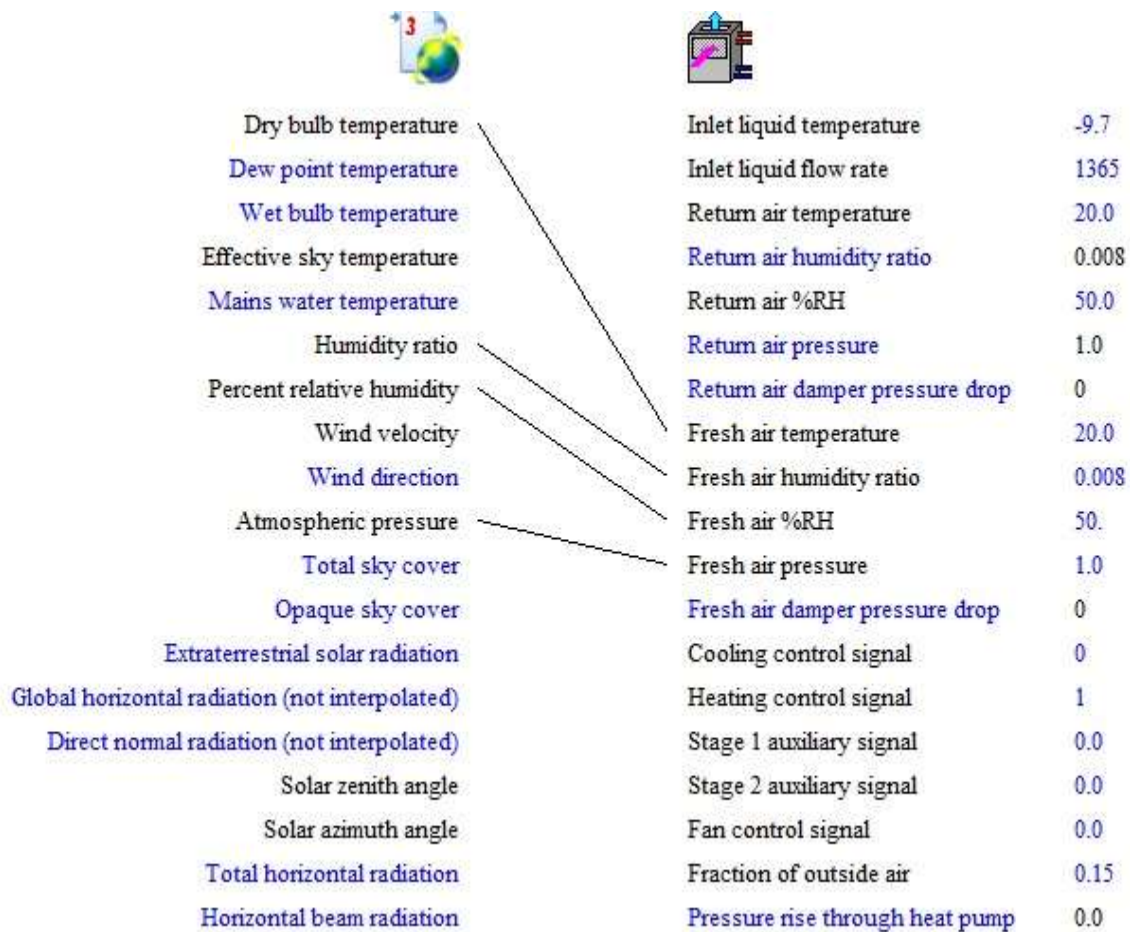


Figure 18. Connection between weather and WSHP

Thermostats play a primary role in regulating HVAC system operation to maintain the prescribed setpoint temperature. In this project, component Type 108—a five-stage thermostat—is implemented, incorporating a three-stage heating source and a two-stage cooling source.

The number of oscillations in this model is restricted to five, which offers two benefits:

1. This approach prevents the model from repeatedly switching between on and off within a single time step, thereby enhancing numerical stability and supporting simulation convergence.
2. Since the number is odd, two consecutive time steps will always result in different end conditions. For example, if the thermostat is active during one time step, it will be inactive in the subsequent time step, thereby preventing simultaneous on–off switching within a single time step.

Another important characteristic of thermostats is the deadband. For instance, when the setpoint temperature is 24 °C and the deadband is 2 °C, the cooling system activates at 24 °C and deactivates at 22 °C. This control strategy reduces excessive cycling by preventing frequent on–off operation of the system.

Connecting the thermostat to the building model (Type 56), as shown in the figure below, enables the definition of various setpoints.

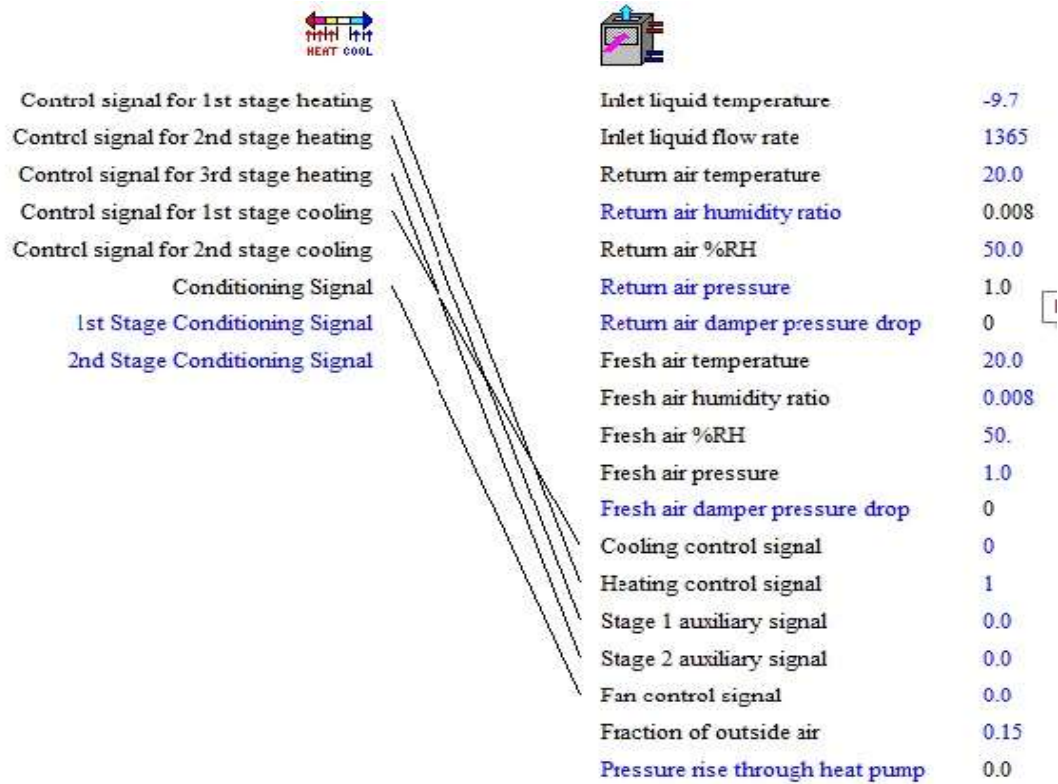


Figure 19. Connection 5 stages thermostat and the WSHP

The thermostat setpoints for the five zones are specified as presented below.

(Review3) THR

Parameter	Input	Output	Comment	
Name	Value	Unit	More	Macro
1 Monitoring temperature	20.0	C	More...	<input checked="" type="checkbox"/>
2 1st stage heating setpoint	20.0	C	More...	<input checked="" type="checkbox"/>
3 2nd stage heating setpoint	18.0	C	More...	<input checked="" type="checkbox"/>
4 3rd stage heating setpoint	16.0	C	More...	<input checked="" type="checkbox"/>
5 1st stage cooling setpoint	24.0	C	More...	<input checked="" type="checkbox"/>
6 2nd stage cooling setpoint	26.0	C	More...	<input checked="" type="checkbox"/>

Figure 20. Setpoints of the thermostat

The selected setpoints are broadly aligned with the values applied in the building.



Figure 21. Setpoints at the building

An essential aspect of designing the water-source heat pump involves controlling the direction of water circulation during both the heating and cooling seasons. This can be achieved by defining specific equations that govern the flow direction.

Within this heat-cool control block, three independent variables and five dependent equations are established to regulate the operation of the heating and cooling pumps, as well as the direction of water circulation.

The independent variables are:

- CoolingSeasonIndicator – from the weather component
- ConditioningSignal – from the thermostat component
- ControlSignalCooling – from the thermostat component

The dependent equations are:

CoolMode = CoolingSeasonInd

HeatingPump = LT(CoolMode,0.5)*GT(ConditioningSignal,0.5) (15)

$$\text{CoolingPump} = \text{GT}(\text{CoolMode}, 0.5) * \text{GT}(\text{ConditioningSignal}, 0.5) \quad (16)$$

$$\text{PumpSelect} = \text{GT}(\text{CoolMode}, 0.5) \quad (17)$$

$$\text{BRcir} = \text{GT}(\text{CoolMode}, 0.5) - \text{LE}(\text{CoolMode}, 0.5) \quad (18)$$

The interpretation of these equations is presented as follows:

It is possible to set CoolMode equal to either ControlSignalCooling or CoolingSeasonIndicator. In both cases, the control signal will produce a value of either 0 or 1. In Equation (15), which governs the operation of the heating pump, the first term ensures that the output equals unity when the CoolMode value is less than 0.5, indicating that the system is not operating in cooling mode. If, in addition, the second term—representing the ConditioningSignal—exceeds 0.5, the combined effect of the equation activates the heating pump, thereby placing the system in heating mode.

In Equation (16), the first term evaluates to true when CoolMode is active (equal to 1), while the second term is satisfied when the ConditioningSignal exceeds 0.5. Under these conditions, the system operates in cooling mode. The equation (18) simply determines whether the system is operating in heating or cooling mode in order to control the flow divider and ensure the correct direction of fluid flow. The final equation defines the

direction of fluid circulation within the boreholes, which is reversed between winter and summer operation. Figure 24 illustrates the boreholes and the connecting pipe network.

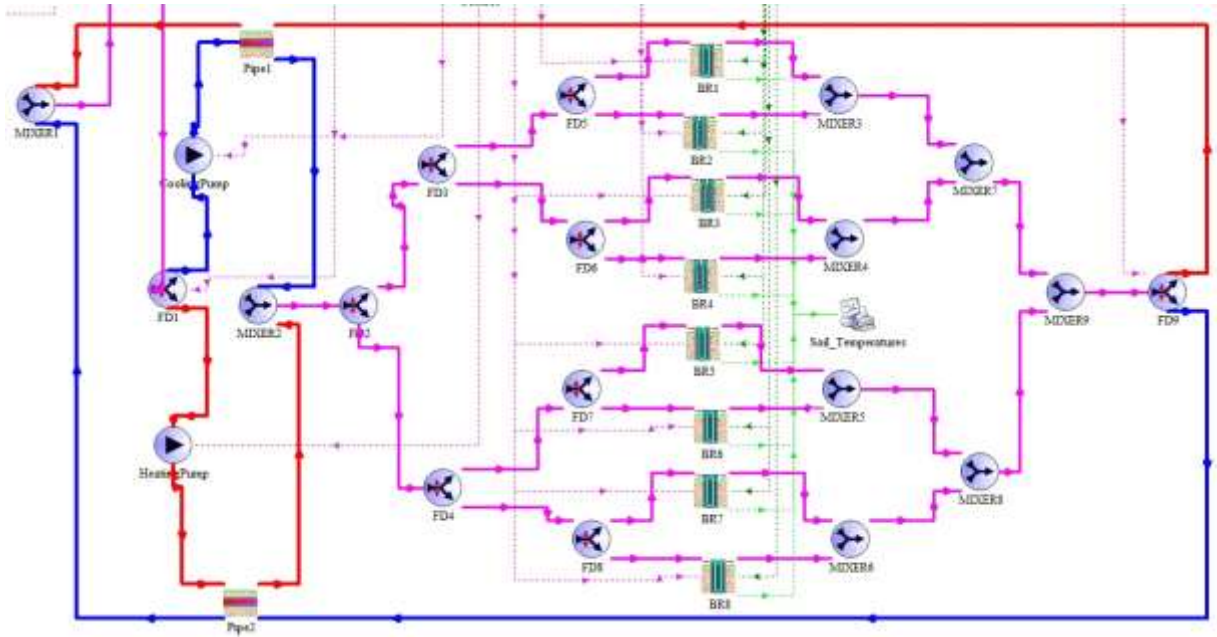


Figure 22. Boreholes

4 Results and discussion

4.1 Temperature Control

The figure 25 displays the temperatures of five different zones in the building during January in Vaasa.

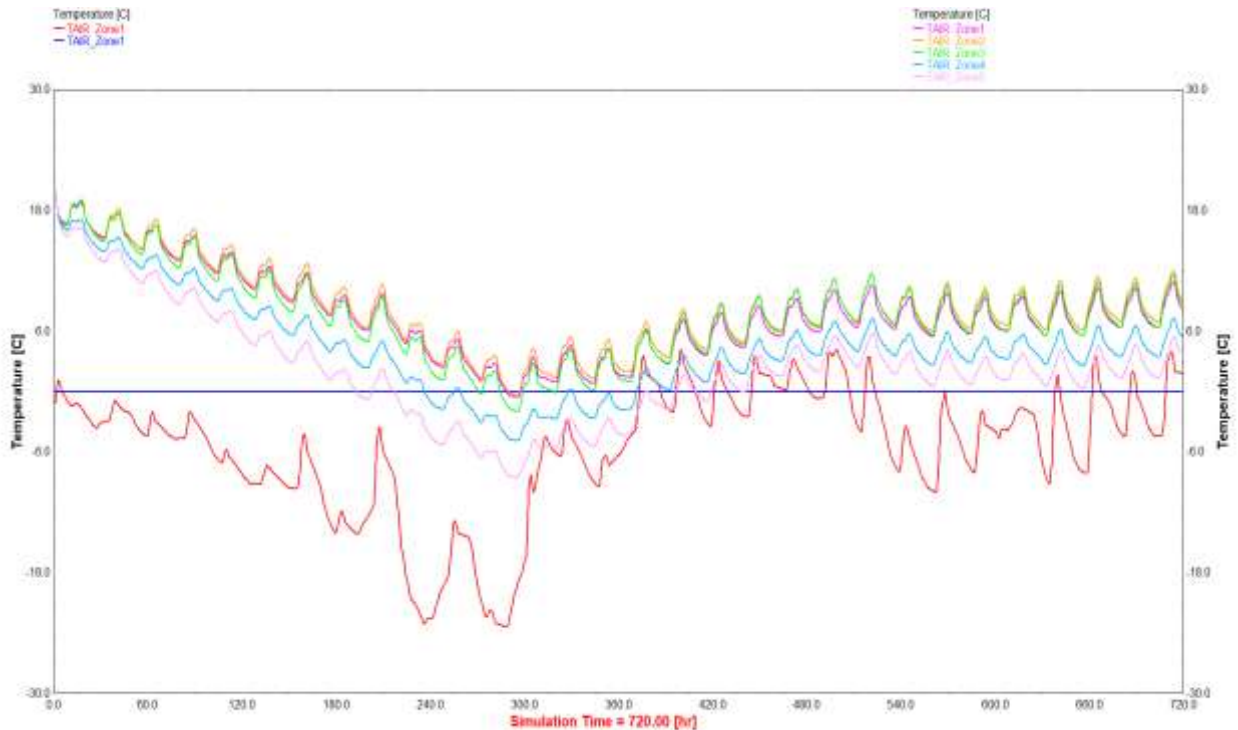


Figure 23. Temperature of the zones and the ambient in January

As is clear, the temperatures are not controlled by the water source heat pump in the figure 25. The temperature curves approximately reach the ambient temperature. Now, by connecting the water source heat pump to the building, the first zone temperature is controlled by the heat pump.

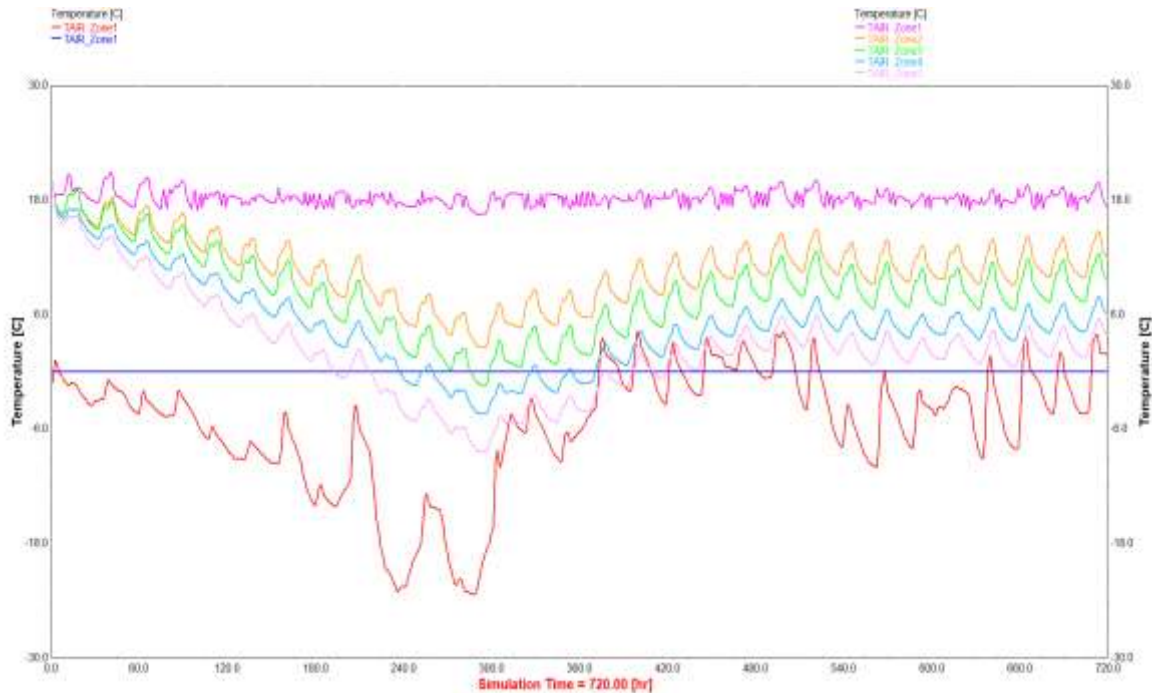


Figure 24. Temperature of the zone1 is controlled by WSHP

By comparing the two figures, it is clear that the temperature of Zone 1 is controlled by the heat pump. It is also evident that the temperature of Zone 1 affects the temperatures of the other zones, since the adjacent boundary condition is defined for them. Zone 2 is affected more because it shares a larger common boundary with Zone 1. In figure 26, the temperature of Zone 2 drops close to 0 °C, while in the next figure it does not. In fact, in both situations Zone 2 is not controlled by the heat pump; however, due to the boundary conditions defined for it, it is affected by the temperature of Zone 1.

4.2 Boreholes Temperatures:

Another result of the simulation is the soil temperature profile, which illustrates the direction of heat transfer. The boreholes act as seasonal thermal storage: in warm weather (summer), the soil temperature rises as heat is transferred into the ground, while in winter the soil temperature decreases as heat is extracted from the ground. In figure 27, the simulation (that is in the 5th year) shows that around mid-year (~38,700 h, summer) the cooling load dominates; consequently, the average soil temperature rises as heat is injected into the ground.

Ring 1: the soil zone closest to the borehole wall (right next to the grout/pipe).

Ring 2: the next radial zone, a bit further out.

Ring 3: even further away from the borehole.

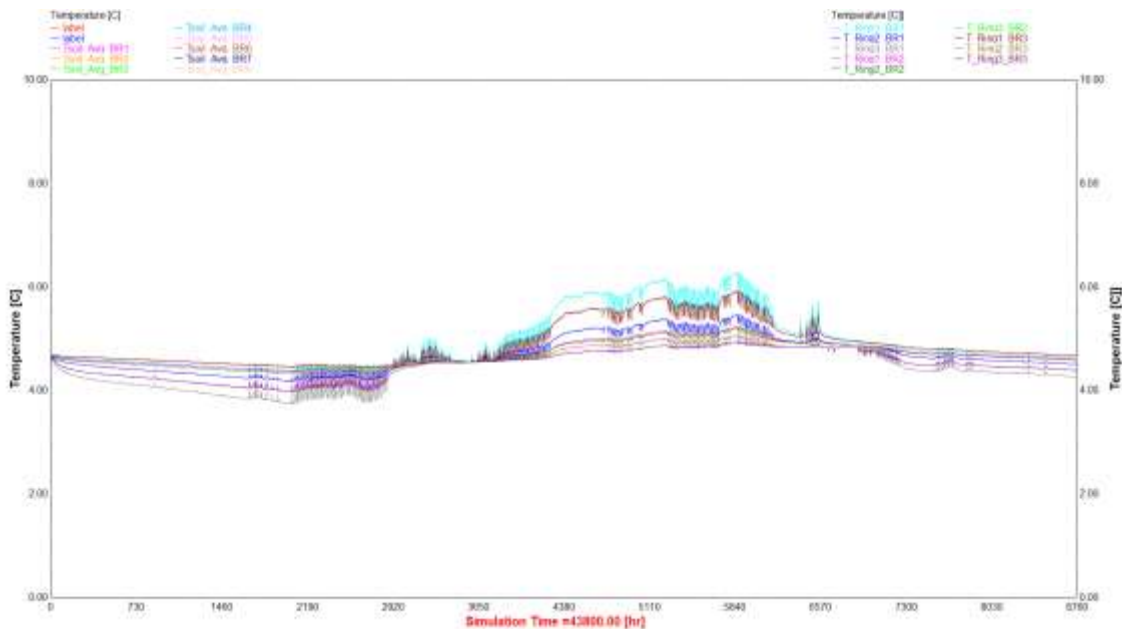


Figure 25. Soil temperatures in boreholes during the first years

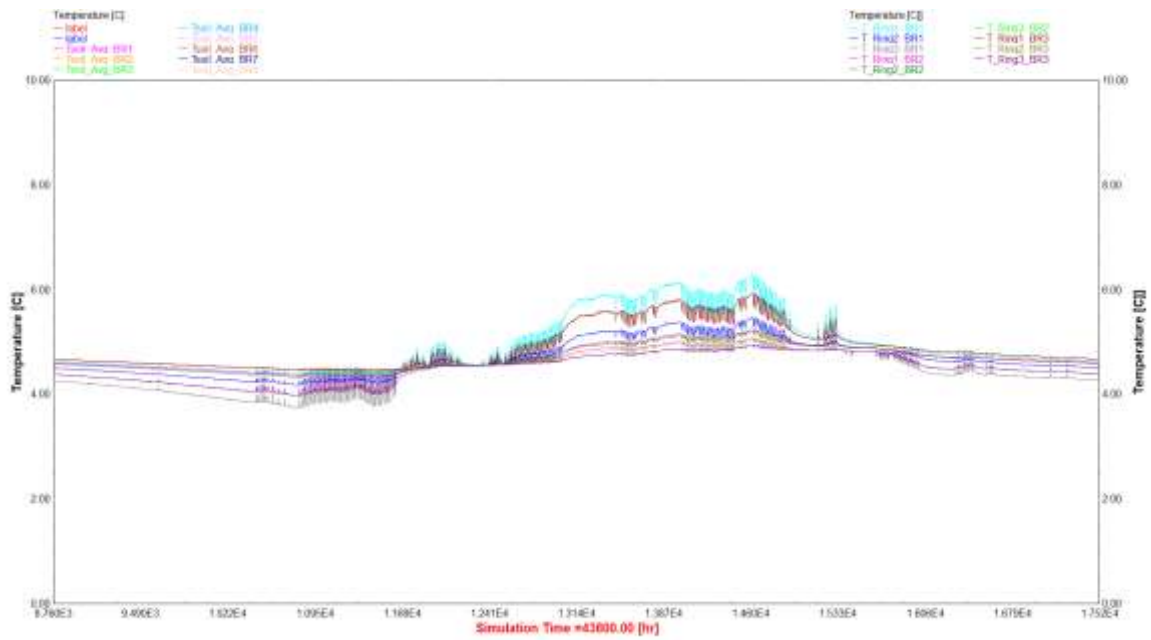


Figure 26. Soil temperatures in boreholes after 2 years

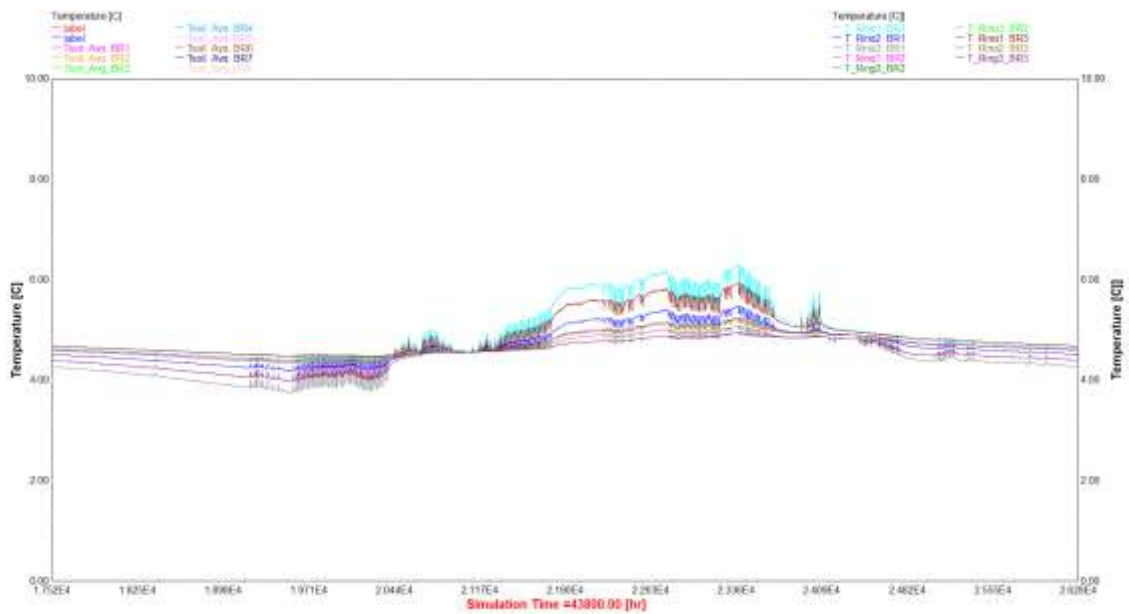


Figure 27. Soil temperatures in boreholes after 3 years

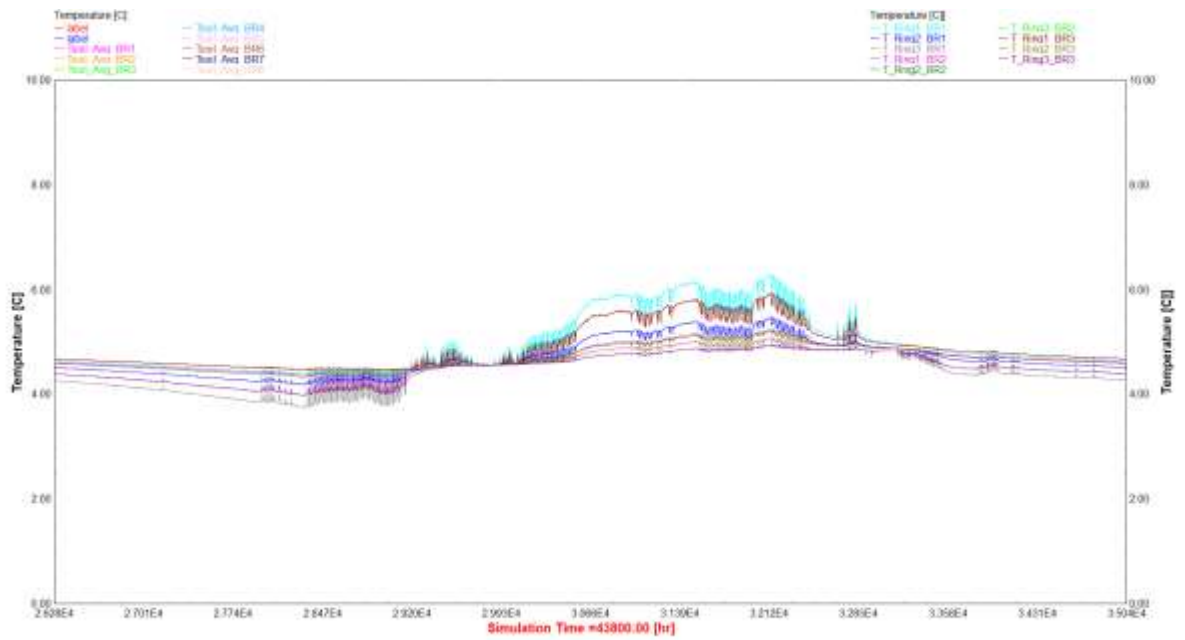


Figure 28. Soil temperatures in boreholes after 4 years

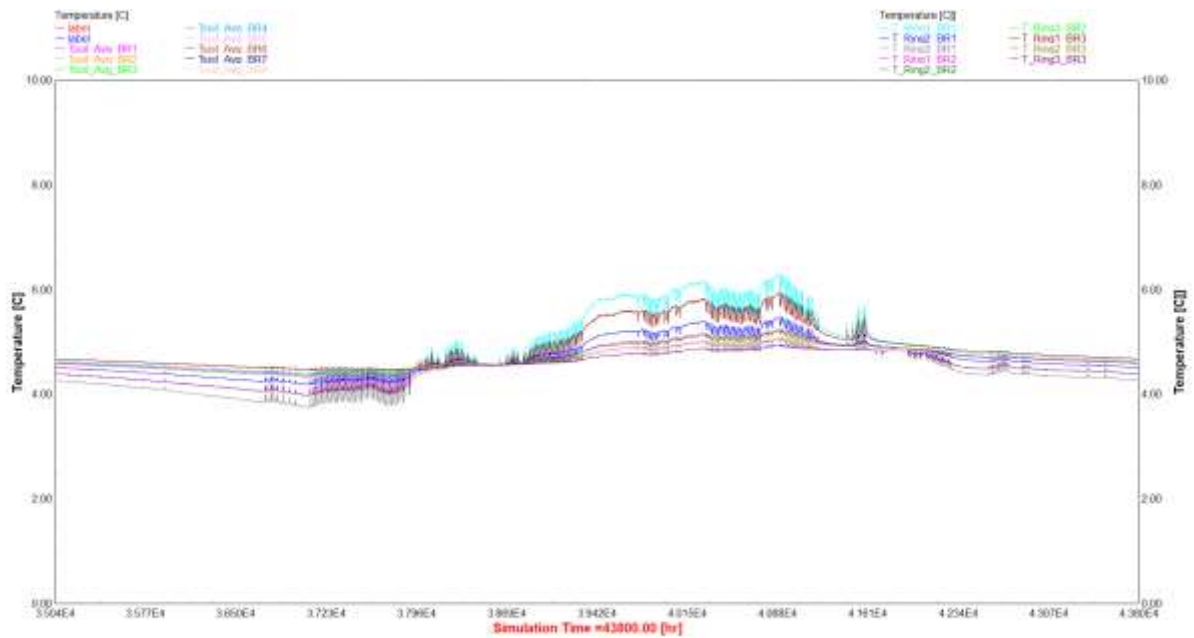


Figure 29. Soil temperatures in boreholes after 5 years

4.3 Heating and Cooling Mode:

The system starts with the heating pump in January, then switches to the cooling pump at around 3,700 hours, and back to the heating pump at 6,500 hours, continuing in heating mode until the end of the year.

0–3,700 h (~Jan–May): Heating pump active.

3,700–6,500 h (~May–Sep): Cooling pump active.

6,500–8,760 h (~Sep–Dec): Heating pump again until year-end.

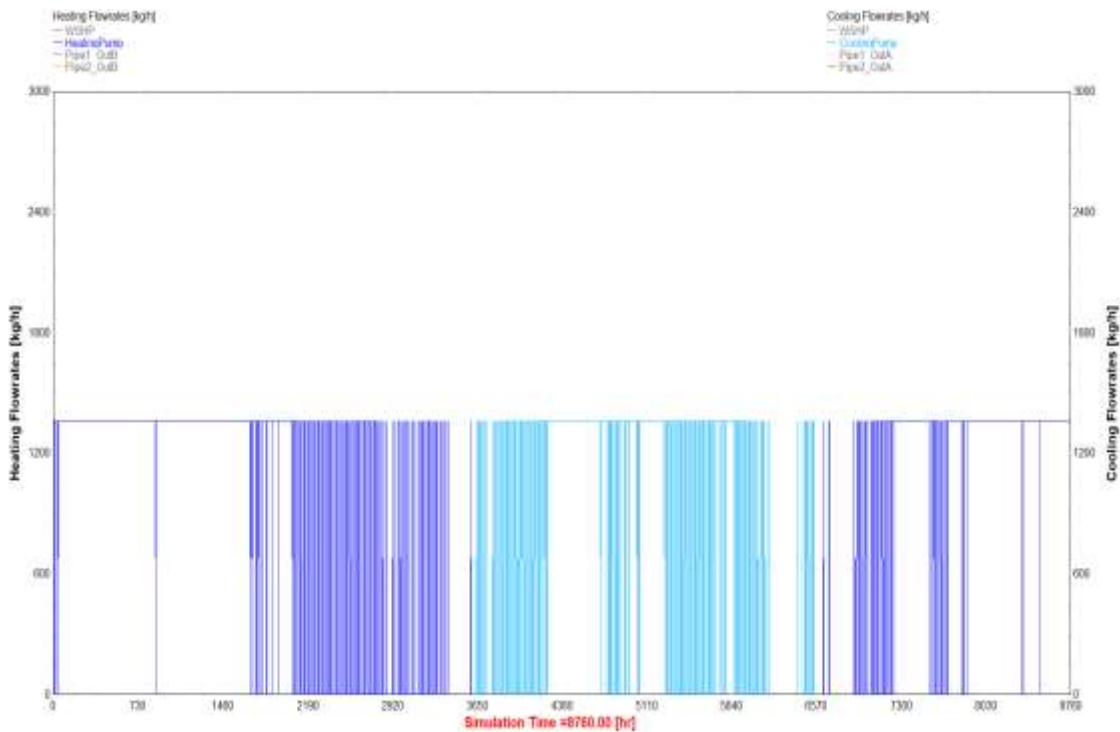


Figure 30. Heating and Cooling Mode

5 Optimization of COP of heat pump:

To enable the optimization process, the original TRNSYS model was extended by integrating the TRNOPT component, which provides an interface between TRNSYS and the external optimization engine GenOpt. Since TRNSYS does not perform numerical optimization internally, the optimization procedure relies on GenOpt, which is executed through a Java-based environment. Once this coupling is established, design variables can be systematically modified and evaluated based on their impact on system performance. In the present study, the borehole depth and the number of boreholes were selected as optimization variables, as these parameters directly influence the thermal interaction between the ground and the water-source heat pump.

The optimization objective was to maximize the coefficient of performance (COP) of the heat pump. Because the optimization routine in TrnOpt is formulated as a minimization problem, the COP was introduced into the cost function with a negative sign, thereby transforming the maximization task into an equivalent minimization problem. A coordinate search algorithm was employed due to its robustness and suitability for nonlinear energy system models. Borehole depth was treated as a continuous variable within practical bounds representative of typical Nordic geothermal installations, while mesh-size refinement and iteration limits were applied to ensure convergence. The results show that increasing borehole depth and borehole count improves COP by reducing ground temperature fluctuations; however, the incremental benefit becomes progressively smaller beyond approximately 200 m, indicating diminishing returns. This confirms that an optimal configuration exists in which performance improvements must be balanced against increased system complexity and installation cost.

$$\text{COP} = \frac{\text{Total Heating Rate (or Total Cooling Rate)}}{\text{Heat pump power}}$$

The results in Table 7 indicate that increasing the borehole depth leads to higher COP values.

Table 9. Optimization results

Initial Depth	Min. Depth	Max. Depth	Opt. Depth	COP
50	50	60	60	1.9641535
50	50	100	100	1.9947454
50	50	150	150	2.0028233
50	50	200	200	2.0035383
50	50	250	250	2.0070533
50	50	300	300	2.0071315

Figure 31 shows the direct results of the optimization, where the depth of boreholes varies from 50 m to 200 m in steps of 5

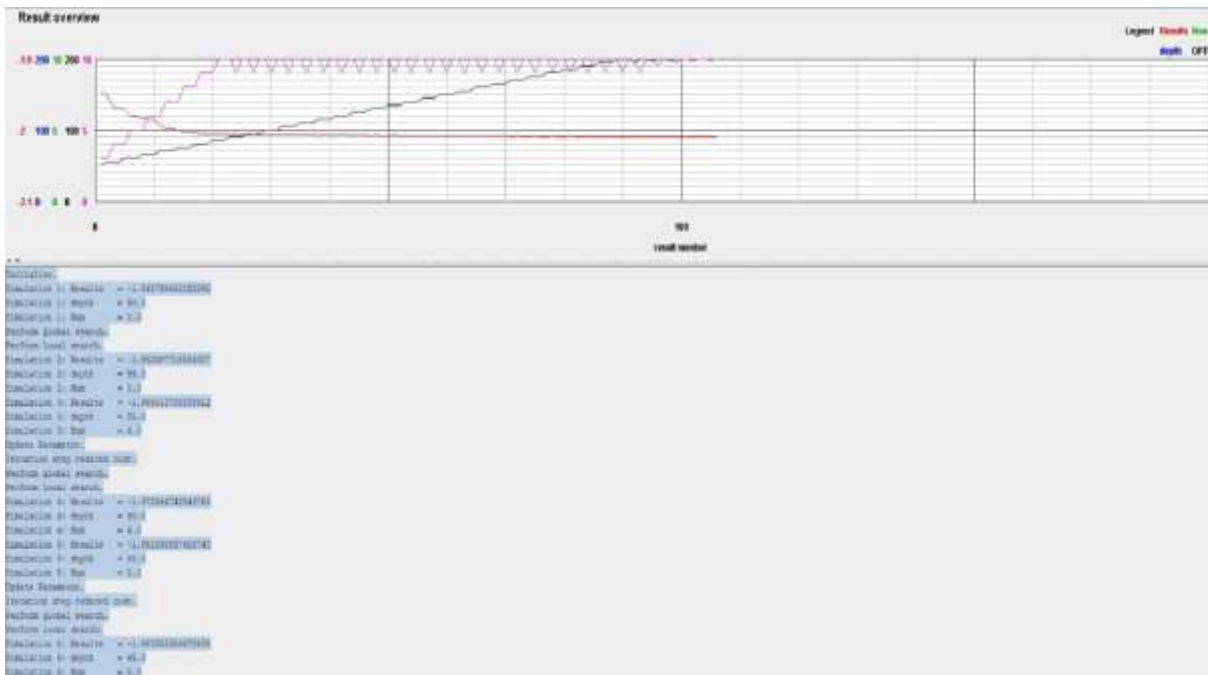


Figure 31. Optimization

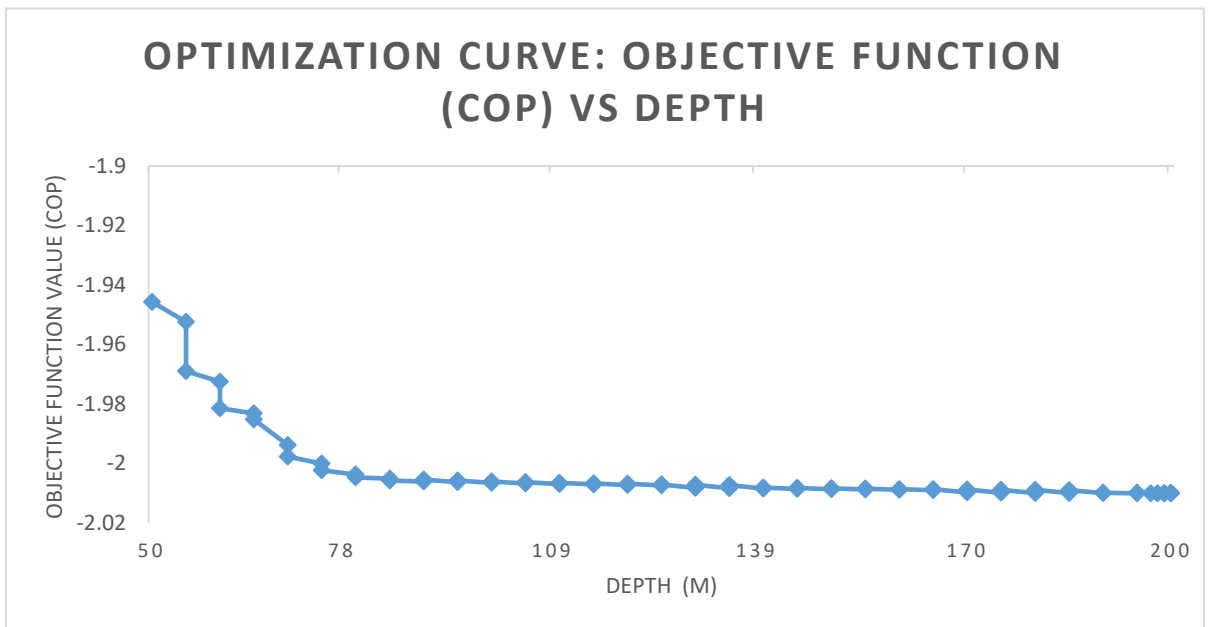


Figure 32. Objective function (cop) vs depth

6 Validation:

For validation the table 8 should be used.

Sum of all the annual Heating Loads (kJ) across the 5 zones:

Table 10. Heating loads for each zone

Unit	KJ	KJ	KJ	KJ	KJ
Period	Q_Heat_Z1	Q_Heat_Z2	Q_Heat_Z3	Q_Heat_Z4	Q_Heat_Z5
8760 h	2.05E+08	1.20E+08	2.39E+08	1.59E+08	5.01E+08
Sum of all Heating Load			1,222,743,521 KJ		

Sum of all the annual Cooling Loads (kJ) across the 5 zones:

Table 11. cooling loads for each zone

Unit	KJ	KJ	KJ	KJ	KJ
Period	Q_Cool_Z1	Q_Cool_Z2	Q_Cool_Z3	Q_Cool_Z4	Q_Cool_Z5
8760 h	1.35E+07	2.62E+07	4.16E+07	1.36E+06	1.98E+06
Sum of all Cooling Load			84,620,012 KJ		

Total loads (kJ):

$$Q_{\text{tot}} = Q_{\text{heat,tot}} + Q_{\text{cool,tot}} = 1,307,363,532.806 \text{ kJ}$$

To convert kJ to kWh, The number should be divided by 3600 since 1 kWh=3600 kJ

$$Q_{\text{total}}(\text{KWh}) = \frac{1,307,363,532.806}{3600} = 363,157 \text{ kWh/a}$$

Rounded to whole kWh:

- Heating \approx 339,651 kWh/a
- Cooling \approx 23,506 kWh/a
- Total \approx 363,157 kWh/a












Report total loads demand (Energiaselvitys, EnergyLab Vaasa 2015):

$$\text{space heating} + \text{supply-air heating} + \text{cooling} = 132.526 \text{ kWh/a} + 173.081 \text{ kWh/a} + 15,585 \text{ kWh/a} = 321,192 \text{ kWh/a}$$

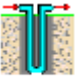


Difference = 363,157 kWh/a - 321,192 kWh/a = 41,965 kWh/a (13 %) This difference could be due to various reasons such as internal gains, ventilation schedule, and infiltration rate.

7 Component List

The following component types from the TRNSYS library were used in this simulation:

	Type14h Forcing Function General		Type41d Unique days and Holidays
	Type56 Multi_Zone Building		Equa Equation
	Type114 Single Speed Pump		Type11f Flow Diverter
	Type143 Water source Heat Pump		Type11d Control Flow Mixer
	Type108 5 Stages Room Thermostat		Type15-TMY3 Weather data reading
	Type65c Online Ploter with File		

The following component types from the TESS library were used in this simulation:

	Type557a_v2a Geothermal Heat Exchanger U-Tube		TRNOPT Optimization
	Type952a_v2a Buried Pipe		

8 Summary

The thesis investigates the application of renewable energy systems, such as geothermal energy, in buildings. For this purpose, a building was chosen as a representative (reference) building. The primary aim is to determine the total cooling and heating loads of the building. The building is divided into five zones, each treated as a lumped system, and these zones are connected to a water-source heat pump. The water-source heat pump is linked to borehole thermal heat exchangers which provide a stable thermal reservoir. This thesis contributes to understanding the dynamic simulation of geothermal energy systems integrated into buildings.

The study begins with creating a 3D model of the building in SketchUp. This is not a typical architectural 3D model; instead, the model was created using TRNSYS3D, a plug-in for SketchUp. In this model, the walls, floors, and roof are defined as either external or adjacent surfaces. As a result, we obtain a lumped system that can act as a thermal mass in direct contact with the outside temperature. After that, the model is imported into TRNSYS, an energy simulation program, using component type 56. The materials of the external and internal walls, the external roof, adjacent ceiling, ground floor, and window glazing are then defined, so that the heat transfer rate through the envelope of each zone can be determined. All operating regimes of the building, including ventilation, infiltration rate, and internal gains such as people, lighting, and equipment, are also specified. As the weather component represents the most significant driving force in the simulation, standard TMY3 format weather data is used. In this way, the total cooling and heating loads are calculated to support the selection of an appropriate HVAC system.

To compensate for the thermal loads, a combination of a water-source heat pump and a series of boreholes is used. Flow dividers, mixers, pumps, and pipe components are employed to simulate the energy generation system for meeting the load of the building. The most important component is the five-stage thermostat, which regulates the operation of the water-source heat pump based on the zone temperatures. In addition, an equation

is introduced to reverse the circulation of the fluid in winter and summer, therefore, controlling the direction of water flow through the boreholes.

The results accurately predict the load of the building and demonstrate how the water-source heat pump can compensate the thermal demand. The heating and cooling modes can also be switched according to the cooling seasonal indicator. The results also showed that the geothermal system operates in clear seasonal cycles: heat is extracted from the ground during winter and injected back during summer. Importantly, the soil temperature returned close to its initial value at the end of the year, indicating a state of thermal balance and confirming the long-term feasibility of the system.

Overall, this study confirms that geothermal heat pump systems with borehole energy storage provide a reliable, efficient, and environmentally sustainable solution for modern buildings. The findings highlight the importance of accurate modeling of both building loads and subsurface conditions in order to achieve optimal system design. By demonstrating the technical viability of such systems, this work supports the role of geothermal energy in reducing carbon emissions and advancing Europe's transition towards low-carbon, energy-efficient building infrastructure.

9 Conclusion

This thesis focuses on the simulation of renewable energy-integrated building energy systems, using the building as a representative office building. The objective is to model and analyze the heating and cooling performance of the building and its interaction with geothermal borehole heat exchangers.

The results clearly demonstrate that a water-source heat pump, supported by borehole exchangers, can effectively cover the heating and cooling needs of a large building in a cold Nordic climate. The simulations confirmed that the building's thermal demand can be met while maintaining indoor comfort through temperature-based control, with heating in winter and cooling in summer provided by the same system.

The seasonal performance of the boreholes was shown to be well-balanced: soil temperatures decreased during winter due to heat extraction but recovered during summer as excess heat was reinjected. Importantly, the system reached thermal balance over repeated years of operation, confirming its long-term sustainability. The results also revealed that the total simulated building energy demand was higher than the measured consumption, which is likely due to uncertainties in modeling assumptions such as internal gains, infiltration, and ventilation schedules. Nevertheless, the dynamic behavior of the system was well captured, and the optimization study further highlighted that borehole depth influence the coefficient of performance (COP) of the heat pump.

References

- Akbulut, L., Taşdelen, K., Atılgan, A., Malinowski, M., Çoşgun, A., Şenol, R., Akbulut, A., & Petryk, A. (2025). A Systematic Review of Building Energy Management Systems (BEMS): Sensors, IoT, and AI Integration. In *Preprints: Preprints*.
- Akraminejad, R., Zhao, T., Rezgui, Y., Ghoroghi, A., & Shahbazi Razlighi, Y. (2025). Hybrid Metaheuristic Optimization of HVAC Energy Consumption and Thermal Comfort in an Office Building Using EnergyPlus. *Buildings*, *15*(14), 2568.
- Amarasinghe, I., Liu, T., Stewart, R., & Mostafa, S. (2024). Paving the way for lowering embodied carbon emissions in the building and construction sector. *Clean Technologies and Environmental Policy*, *27*, 1825-1843.
<https://doi.org/10.1007/s10098-024-03023-6>
- Andjelkovic, B., Stojanovic, B., Stojiljković, M., Janevski, J., & Ljubenovic, M. (2012). Thermal mass impact on energy performance of a low, medium and heavy mass building in Belgrade. *Thermal Science*, *16*, 447-459. <https://doi.org/10.2298/TSCI120409182A>
- ASHRAE. (2009). *ASHRAE® HANDBOOK*.
- Barnaby, C. S., Spitler, J., & Xiao, D. (2005). The residential heat balance method for heating and cooling load calculations. *ASHRAE Transactions*, *111*, 308-319.
- Canale, L., Di Fazio, A. R., Russo, M., Frattolillo, A., & Dell'Isola, M. (2021). An Overview on Functional Integration of Hybrid Renewable Energy Systems in Multi-Energy Buildings. *Energies*, *14*(4), 1078.
- Cao, R., Hao, Y., Li, Y., & Liao, W. (2025). Emerging trends in lifecycle assessment of building construction for greenhouse gas control: implications for capacity building. *Discover Applied Sciences*, *7*. <https://doi.org/10.1007/s42452-025-06853-1>
- Castro-García, M. P., Norriella-Llaneza, S., Fernández-González, T., Centeno-Idiáñez, Y., & Alonso-Sánchez, T. (2025). Modeling Thermal Interference Between Shallow Geothermal Boreholes Using TRNSYS: Application to the Q-Thermie-Unioivi Boreholes (Asturias, Spain). *Applied Sciences*, *15*(10), 5591.

- Cazorla-Marín, A., Montagud-Montalvá, C., Tinti, F., & Corberán, J. M. (2020). A novel TRNSYS type of a coaxial borehole heat exchanger for both short and mid term simulations: B2G model. *Applied Thermal Engineering*, *164*, 114500. <https://doi.org/https://doi.org/10.1016/j.applthermaleng.2019.114500>
- Cheng, S., Tekler, Z. D., Jia, H., Li, W., & Chong, A. (2024). Evaluating different levels of information on the calibration of building energy simulation models. *Building Simulation*, *17*(4), 657-676. <https://doi.org/10.1007/s12273-024-1115-8>
- Christodoulides, P., Christou, C., & Florides, G. A. (2024). Ground Source Heat Pumps in Buildings Revisited and Prospects. *Energies*, *17*(13), 3329.
- Constantinou, S., Al-Naemi, F., Alrashidi, H., Mallick, T., & Issa, W. (2023). A review on technological and urban sustainability perspectives of advanced building - integrated photovoltaics. *Energy Science & Engineering*, *12*. <https://doi.org/10.1002/ese3.1639>
- da Silva, P. P., Neto, A. H., & Sauer, I. L. (2021). Evaluation of Model Calibration Method for Simulation Performance of a Public Hospital in Brazil. *Energies*, *14*(13), 3791.
- De Rosa, M., Ruiz-Calvo, F., Corberan, J., Montagud, C., & Tagliafico, L. A. (2015). A novel TRNSYS type for short-term borehole heat exchanger simulation: B2G model. *Energy Conversion and Management*, *100*, 347-357. <https://doi.org/10.1016/j.encoman.2015.05.021>
- Drgoňa, J., Arroyo, J., Cupeiro, I., Blum, D., Arendt, K., Kim, D., Olle, E., Oravec, J., Wetter, M., Vrabie, D., & Helsen, L. (2020). All you need to know about model predictive control for buildings. *Annual Reviews in Control*, *50*. <https://doi.org/10.1016/j.arcontrol.2020.09.001>
- Eze, F. C. (2024). Modeling and Simlation of Solar-Assisted Daul-Source Heat Pump Syedtem with Underground Thermal Storage for Space Heating and Cooling
- Fan, Y., & Fang, C. (2023). GHG emissions and energy consumption of residential buildings- a systematic review and meta-analysis. *Environ Monit Assess*, *195*(7), 885. <https://doi.org/10.1007/s10661-023-11515-z>

Filali, F., & Chafi, F. (2025). Energy consumption and CO₂ emissions in buildings: a bibliometric review of trends, challenges, and future directions. *Journal of the Croatian Association of Civil Engineers*, 77, 367-380.

<https://doi.org/10.14256/JCE.4264.2025>

Finamore, M., & Oltean-Dumbrava, C. (2024). Circular Economy in Construction - Findings from a Literature Review. *Heliyon*, 10, e34647.

<https://doi.org/10.1016/j.heliyon.2024.e34647>

Fouad, H., Mahmoud, A., & Moussa, R. (2024). The effectiveness of geothermal systems in cooling residential buildings: a case study of a residential building in Alexandria, Egypt. *Journal of Engineering and Applied Science*, 71.

<https://doi.org/10.1186/s44147-024-00378-x>

Gholami, M., Torreggiani, D., Tassinari, P., & Barbaresi, A. (2021). Narrowing uncertainties in forecasting urban building energy demand through an optimal archotyping method. *Renewable and Sustainable Energy Reviews*, 148, 111312.

<https://doi.org/https://doi.org/10.1016/j.rser.2021.111312>

Goudarzi, N., Talebi, S., Rezaei Ochbelagh, D., & Sadrizadeh, S. (2023). New Algorithm Development for Real-Time Dynamic Simulation of Thermal–Hydraulic

Grids and Artificial Intelligence–Assisted Hierarchical Control of Integrated

Concentrated Solar Power, Steam Rankine Cycle, and High-Temperature Steam

Electrolysis Systems.

Guo, F., Miao, S., Xu, S., Luo, M., Dong, J., & Zhang, H. (2025). Multi-Objective Optimization Design for Cold-Region Office Buildings Balancing Outdoor Thermal Comfort and Building Energy Consumption. *Energies*, 18(1), 62.

Hannan, M. A., Faisal, M., Ker, P. J., Mun, L. H., Parvin, K., Mahlia, T. M. I., & Blaabjerg, F. (2018). A Review of Internet of Energy Based Building Energy Management Systems: Issues and Recommendations. *IEEE Access*, 6, 38997-39014.

<https://doi.org/10.1109/ACCESS.2018.2852811>

- Hossain, J., Kadir, A. F. A., Hanafi, A. N., Shareef, H., Khatib, T., Baharin, K. A., & Sulaima, M. F. (2023). A Review on Optimal Energy Management in Commercial Buildings. *Energies*, *16*(4), 1609.
- Hu, X. (2025). Holistic renovation strategies for cold climate buildings: simulation-based insights into decarbonization and cost-effectiveness.
- Kim, H., Kim, J., & Yeo, M. (2022). Thermal Bridge Modeling According to Time-Varying Indoor Temperature for Dynamic Building Energy Simulation Using System Identification. *Buildings*, *12*(12), 2178.
- Kirschstein, X., Ohagen, M., Reber, J., & Hübler, C. (2025). Development and validation of a new model for system-integrated shallow borehole heat exchanger fields with irregular geometry. *Geothermics*, *134*, 103481.
<https://doi.org/https://doi.org/10.1016/j.geothermics.2025.103481>
- Kong, Q., Feng, J., Yang, C., Miao, Z., & He, X. (2017). Numerical Simulation of a Radiant Floor Cooling Office Based on CFD-BES Coupling and FEM. *Energy Procedia*, *105*, 3577-3583. <https://doi.org/https://doi.org/10.1016/j.egypro.2017.03.825>
- Kozlovska, M., Petkanic, S., Vranay, F., & Vranay, D. (2023). Enhancing Energy Efficiency and Building Performance through BEMS-BIM Integration. *Energies*, *16*(17), 6327.
- Kvalsvik, K. H., Ramstad, R. K., Holmberg, H., & Kocbach, J. (2025). Measurements and simulations of high temperature borehole thermal energy storage in Drammen, Norway - evaluation of thermal losses and thermal barrier. *Geothermics*, *125*, 103192. <https://doi.org/https://doi.org/10.1016/j.geothermics.2024.103192>
- Liu, M., Zhang, L., Chen, J., Chen, W.-A., Yang, Z., Lo, J., Wen, J., & O'Neill, Z. (2025). Large language models for building energy applications: Opportunities and challenges. *Building Simulation*, *18*. <https://doi.org/10.1007/s12273-025-1235-9>
- Liu, Y., Wang, W., Huang, Y., Song, J., & Zhou, Z. (2024). Energy Performance Analysis and Study of an Office Building in an Extremely Hot and Cold Region. *Sustainability*, *16*(2), 572.

- Ma, M., Zhang, S., Liu, J., Yan, R., Cai, W., Zhou, N., & Yan, J. (2025). Building floorspace and stock measurement: A review of global efforts, knowledge gaps, and research priorities. *Nexus*, 2(3). <https://doi.org/10.1016/j.nexs.2025.100075>
- Maduta, C., D'Agostino, D., Tsemekidi-Tzeiranaki, S., & Castellazzi, L. (2025). From Nearly Zero-Energy Buildings (NZEBS) to Zero-Emission Buildings (ZEBs): Current status and future perspectives. *Energy and Buildings*, 328, 115133.
<https://doi.org/https://doi.org/10.1016/j.enbuild.2024.115133>
- Magrini, A., Lentini, G., Cuman, S., Bodrato, A., & Marengo, L. (2020). From Nearly Zero Energy Buildings (NZEBS) to Positive Energy Buildings (PEB): the next challenge - The most recent European trends with some notes on the energy analysis of a forerunner PEB example. *Developments in the Built Environment*, 3, 100019.
<https://doi.org/10.1016/j.dibe.2020.100019>
- Manfren, M., Gonzalez-Carreon, K. M., & James, P. A. B. (2024). Interpretable Data-Driven Methods for Building Energy Modelling—A Review of Critical Connections and Gaps. *Energies*, 17(4), 881.
- Marttila, M. (2025). *Sustainable and Profitable Office Retrofits in Finland: A Development Perspective*
- Meiers, J., & Frey, G. (2025). Interfacing TRNSYS with MATLAB for Building Energy System Optimization. *Energies*, 18(2), 255.
- Michailidis, P., Michailidis, I., & Kosmatopoulos, E. (2025). Reinforcement Learning for Optimizing Renewable Energy Utilization in Buildings: A Review on Applications and Innovations. *Energies*, 18(7), 1724.
- Mohammadzadeh Bina, S., Fujii, H., Kosukegawa, H., & Inagaki, F. (2024). A predictive model of long-term performance assessment of Ground Source Heat Pump (GSHP) systems in Japanese regions. *Geothermics*, 119, 102955.
<https://doi.org/https://doi.org/10.1016/j.geothermics.2024.102955>

- Muslim, S. (2021). EnergyPlus-Towards the Selection of Right Simulation Tool for Building Energy and Power Systems Research. *Journal of Energy and Power Technology*, 3, 1-1. <https://doi.org/10.21926/jept.2103034>
- Olatunde, T., Okwandu, A., Akande, D., & Sikhakhane, Z. (2024). Review of energy-efficient HVAC technologies for sustainable buildings. *International Journal of Science and Technology Research Archive*, 6, 012-020.
<https://doi.org/10.53771/ijstra.2024.6.2.0039>
- Pachano, J. E., & Bandera, C. F. (2021). Multi-step building energy model calibration process based on measured data. *Energy and Buildings*, 252, 111380.
<https://doi.org/https://doi.org/10.1016/j.enbuild.2021.111380>
- Paola Rocca, V. A., Cortella, G., & D'Agaro, P. Simplified and Fully Detailed Dynamic Building Energy Simulation Tools Compared to Monitored Data for a Single-Family NZEB House.
- Reddy, V. J., Hariram, N. P., Ghazali, M. F., & Kumarasamy, S. (2024). Pathway to Sustainability: An Overview of Renewable Energy Integration in Building Systems. *Sustainability*, 16(2), 638.
- Riazul Jannat Eiva, U., Fahim, T., Islam, S. S., & Ullah, A. (2023). Design, performance, and techno - economic analysis of a rooftop grid - tied PV system for a remotely located building. *IET Renewable Power Generation*, 19, n/a-n/a.
<https://doi.org/10.1049/rpg2.12793>
- Roland, R., Banihashemi, F., & Werner, L. (2022). Sensitivity and uncertainty analysis of combined building energy simulation and life cycle assessment.
- Rotimi, A., Bahadori-Jahromi, A., Mylona, A., Godfrey, P., & Cook, D. (2017). Estimation and Validation of Energy Consumption in UK Existing Hotel Building Using Dynamic Simulation Software. *Sustainability*, 9(8), 1391.
- Salhein, K., Salheen, S. A., Annekaa, A. M., Hawsawi, M., Alhawsawi, E. Y., Kobus, C. J., & Zohdy, M. (2025). A Comprehensive Review of Geothermal Heat Pump Systems. *Processes*, 13(7), 2142.

- Singh, V., Ahirwar, B. K., Paraye, P., Kushwah, S., Patel, A., Nigam, P., Tiwari, R., & Tinnaluri, V. S. N. (2025). A categorical review of advancements, efficiency, and sustainability in solar water heating systems. *Journal of Thermal Analysis and Calorimetry*, 150. <https://doi.org/10.1007/s10973-025-14431-1>
- Sun, Y., Zhao, T., & Lyu, S. (2024). Model-based investigation on building thermal mass utilization and flexibility enhancement of air conditioning loads. *Building Simulation*, 17, 1-20. <https://doi.org/10.1007/s12273-024-1143-4>
- Tejani, A., & Toshiwal, V. (2023). Enhancing Urban Sustainability: Effective Strategies for Combining Renewable Energy with HVAC Systems. 1, 47-60. <https://doi.org/10.56472/25839322/IJAST-V1I1P107>
- Tian, W. (2024). Towards advanced uncertainty and sensitivity analysis of building energy performance using machine learning techniques. *Journal of Building Performance Simulation*, 17, 1-8. <https://doi.org/10.1080/19401493.2024.2387071>
- Tomrukçu, G., Kizildag, H., Avgan, G., Dal, A., Ganiç Sağlam, N., Kalaycıoğlu, E., & Ashrafiyan, T. (2024). A Systematic Approach to Manual Calibration and Validation of Building Energy Simulation. *Smart and Sustainable Built Environment*. <https://doi.org/10.1108/SASBE-10-2023-0296>
- Tozlu, S. (2025). Calibration of building energy simulation models for energy-efficient retrofitting: A residential case study in Samsun-Havza. *International Journal of Energy Studies*, 10, 595-617. <https://doi.org/10.58559/ijes.1623553>
- TRNSYS. (2024). *TRNSYS 18 Tutorials*. In (Version 18)
- Wang, C., Ma, M., Su, Y., Wang, Y., Wang, Y., Chen, Y., Fan, L., Peng, C., & Deng, J. (2025). Research on the operation features and optimization methods of heat pumps coupled with mid-deep borehole heat exchangers: On-site measurements and comparative study. *Energy and Buildings*, 328, 115239. <https://doi.org/https://doi.org/10.1016/j.enbuild.2024.115239>
- Wang, D., Zheng, W., Wang, Z., Wang, Y., Pang, X., & Wang, W. (2023). Comparison of reinforcement learning and model predictive control for building energy system

- optimization. *Applied Thermal Engineering*, 228, 120430.
<https://doi.org/https://doi.org/10.1016/j.applthermaleng.2023.120430>
- Wang, X., Li, T., Yu, Y., Liu, Q., Shi, L., Xia, J., & Mao, Q. (2024). Performance simulation and energy efficiency analysis of multi-energy complementary HVAC system based on TRNSYS. *Applied Thermal Engineering*, 257, 124378.
<https://doi.org/10.1016/j.applthermaleng.2024.124378>
- Wang, X., Li, X., Zhu, X., Wang, H., Qin, H., Dong, Z., Shi, R., & Zhao, P. (2025a). Thermal stability and energy efficiency optimization of ground source heat pump systems: A study on the synergistic energy supply mechanism of pile foundation and medium-deep borehole heat exchangers. *Journal of Building Engineering*, 114195.
<https://doi.org/https://doi.org/10.1016/j.jobe.2025.114195>
- Wang, X., Li, X., Zhu, X., Wang, H., Qin, H., Dong, Z., Shi, R., & Zhao, P. (2025b). Thermal stability and energy efficiency optimization of ground source heat pump systems: A study on the synergistic energy supply mechanism of pile foundation and medium-deep borehole heat exchangers. *Journal of Building Engineering*, 114, 114195.
<https://doi.org/https://doi.org/10.1016/j.jobe.2025.114195>
- Wang, Z., Lu, M., Wang, F., Li, Y., Bai, M., Qin, H., & Ma, Z. (2025). Integrating seasonal borehole thermal energy storage into deep borehole ground source heat pump systems: Dynamic performance analysis under uncertainties. *Energy Conversion and Management*, 341, 120030.
<https://doi.org/https://doi.org/10.1016/j.enconman.2025.120030>
- Xie, Y., & Sun, X. (2025). Smart Implementation and Expectations for Sustainable Buildings: A Scientometric Analysis. *Buildings*, 15(14), 2436.
- Xu, W., Li, J., Zhang, G., Sun, Z., & Li, J. (2025). Research status and future development of the medium-deep geothermal heat pump heating system - A comprehensive review. *Renewable and Sustainable Energy Reviews*, 225, 116141.
<https://doi.org/https://doi.org/10.1016/j.rser.2025.116141>

- Young-seo, Y. (2021). *Uncertainty in Sensitivity of Building Design Variables by Building Usage Scenarios* Seoul National University Graduate School]. <https://hdl.handle.net/10371/178731>
<https://dcollection.snu.ac.kr/common/orgView/000000167766>
- Yu, J., Chang, W.-S., & Dong, Y. (2022). Building Energy Prediction Models and Related Uncertainties: A Review. *Buildings*, 12(8), 1284.
- Zarate Perez, E., Santos-Mejía, C., & Sebastian, R. (2023). *Global trends in building energy management systems (BEMS): A science mapping approach*. <https://doi.org/10.1063/5.0171397>
- Zhang, N., Yang, Q., Chang, X., Yu, Y., Yang, J., & Han, T. (2025). A novel approach for delineating the suitability zone of ground coupled heat pump system and geothermal resource potential in a seasonally frozen region. *Renewable Energy*, 256, 124150. <https://doi.org/https://doi.org/10.1016/j.renene.2025.124150>
- Zhao, Q., Wu, Z., Yu, Y., Wang, T., & Huang, S. (2025). Exploring Carbon Emissions in the Construction Industry: A Review of Accounting Scales, Boundaries, Trends, and Gaps. *Buildings*, 15, 1900. <https://doi.org/10.3390/buildings15111900>